

# 1 Spatial spread of infectious diseases 2 with conditional vector preferences

3 **Frédéric M. Hamelin**<sup>1,\*</sup>, **Frank M. Hilker**<sup>2</sup>, **Yves Dumont**<sup>3,4,5</sup>

4 <sup>1</sup> Institut Agro, Univ Rennes, INRAE, IGEPP, 35000, Rennes, France

5 <sup>2</sup> Institute of Mathematics and Institute of Environmental Systems Research, Osnabrück Uni-  
6 versity, D-49069 Osnabrück, Germany

7 <sup>3</sup> CIRAD, UMR AMAP, 97410 St Pierre, Réunion Island, France

8 <sup>4</sup> AMAP, Univ Montpellier, CIRAD, CNRS, INRAE, IRD, Montpellier, France

9 <sup>5</sup> Department of Mathematics and Applied Mathematics, University of Pretoria, Pretoria,  
10 South Africa

11 \* Corresponding author: frederic.hamelin@institut-agro.fr

12

---

13 **Abstract** We explore the spatial spread of vector-borne infections with  
14 conditional vector preferences, meaning that vectors do not visit hosts at random.  
15 Vectors may be differentially attracted toward infected and uninfected hosts  
16 depending on whether they carry the pathogen or not. The model is expressed as a  
17 system of partial differential equations with vector diffusion. We first study the  
18 non-spatial model. We show that conditional vector preferences alone (in the  
19 absence of any epidemiological feedback on their population dynamics) may result  
20 in bistability between the disease-free equilibrium and an endemic equilibrium. A  
21 backward bifurcation may allow the disease to persist even though its basic  
22 reproductive number is less than one. Bistability can occur only if both infected and  
23 uninfected vectors prefer uninfected hosts. Back to the model with diffusion, we  
24 show that bistability in the local dynamics may generate travelling waves with  
25 either positive or negative spreading speeds, meaning that the disease either  
26 invades or retreats into space. In the monostable case, we show that the disease  
27 spreading speed depends on the preference of uninfected vectors for infected  
28 hosts, but also on the preference of infected vectors for uninfected hosts under  
29 some circumstances (when the spreading speed is not linearly determined). We  
30 discuss the implications of our results for vector-borne plant diseases, which are the  
31 main source of evidence for conditional vector preferences so far.

32

---

33 **Keywords:** vector bias, bistability, backward bifurcation, travelling wave, spread-  
34 ing speed, front reversal, pushed and pulled waves.

## 35 **1 Introduction**

36 Vector-borne diseases are a major concern for human, animal and plant health. Since  
37 Ross' seminal work (1911), most mathematical models of vector-borne infections  
38 consider that vectors visit hosts randomly, independent of their infection status [54,  
39 41]. Spatially explicit models are no exception in this regard [37]. However, growing  
40 evidence shows that many vectors do not visit hosts randomly [22].

41 Vectors may be differentially attracted towards infected and uninfected hosts, in-  
42 dependent of whether or not they carry the pathogen [34, 42, 12]. This is termed  
43 a "vector bias" in the modelling literature [9]. [33] was probably the first to include  
44 such a vector bias in a model. He showed that vector preferences can induce bista-  
45 bility, meaning that the dynamics converge either to a disease-free state or to an  
46 endemic state depending on the initial conditions. However, bistability only occurred  
47 in somewhat special cases in which the vector bias was a function of the fraction of  
48 infected hosts in the population. Later studies generally assumed a constant vec-  
49 tor bias and did not find bistability [30, 9, 53], except when disease-induced host  
50 mortality and immigration were included in the model [7].

51 Spatially explicit models have also been used to explore the consequences of a  
52 vector bias in space. Individual-based models were formulated to investigate the  
53 effect of spatial heterogeneity on the spread of vector-borne diseases with a vector  
54 bias [43, 50]. [9] were probably the first to incorporate a vector bias into a partial  
55 differential equation (PDE) model. They numerically showed that travelling waves  
56 occur, and how their speed can be calculated. Later studies then also considered  
57 a vector bias in PDE models [56, 2]. In particular, [55] also showed the existence  
58 of travelling wave solutions. In these studies [9, 55], the models did not exhibit  
59 bistability, and the travelling waves had positive speeds, meaning that the disease  
60 invades a disease-free spatial domain.

61 Vector preferences, however, may depend on whether or not vectors carry the  
62 pathogen [31, 5, 22, 16, 49, 8]. These are termed "conditional vector preferences".

63 [47] were probably the first to include conditional vector preferences in a model,  
64 but they did not fully analyse the model. In particular, whether or not bistability  
65 can occur was left implicit. In a more general version of the model (accounting  
66 for vector handling times), [22] showed that conditional preferences (in particular a  
67 preference of uninfected vectors for infected hosts) can lead to bistability, provided  
68 vector fecundity depends on host infection status. Similarly, [14] observed multi-  
69 stability in a more complex model accounting for vector population dynamics that  
70 depend on the host infection status. However, whether conditional preferences can  
71 lead to bistability when the vector population dynamics are independent of the host  
72 infection status still remains to be clarified.

73 Bistability may have important implications regarding the spatial spread of the  
74 disease in space. In particular, it is well known [21, 38, 35, 44, 17, 29, 27] that  
75 bistability can give rise to negative wave speeds, meaning in our context that the  
76 disease retreats. This phenomenon is also termed “front reversal”.

77 In this study, we analyse whether and how conditional vector preferences can  
78 give rise to bistability and front reversal in vector-borne diseases. The organisation  
79 of the paper is as follows. In Section 2, we present a spatio-temporal (reaction-  
80 diffusion) model with conditional vector preferences. In Section 3, we provide an  
81 analysis of the temporal (non-spatial) model with some numerical simulations. Then,  
82 in Section 4, we go back to the spatio-temporal model (with diffusion), showing  
83 existence of travelling wave solutions. Numerical simulations illustrate our findings.  
84 Lastly, Section 5 concludes the paper with a discussion.

## 85 **2 Spatio-temporal model**

86 Let  $I(x, t)$  be the infected host density at time  $t$  and location  $x \in \mathbb{R}$ . We adopt a uni-  
87 dimensional representation of space for simplicity. The total host density is assumed  
88 to be a constant  $N$  independent of  $x$ . The local density of uninfected hosts at time  
89  $t$  is therefore  $N - I(x, t)$ . Let  $V(x, t)$  and  $U(x, t)$  be the infected (“viruliferous”) and  
90 uninfected vector densities, respectively. Let  $b$  be the vector “biting” rate. Let  $p$  and  
91  $q$  be the probabilities of pathogen transmission and acquisition, respectively. Let  $r$  be  
92 the removal rate of infected hosts. Infected vectors lose the pathogen at rate  $l$  [10].

93 Let  $m$  be the vector mortality rate. For simplicity, we assume that the vector birth  
 94 rate exactly compensates the mortality rate. In addition, we assume that vectors are  
 95 born uninfected. There is no vertical transmission in either the vector or the host.  
 96 Let  $\alpha$  be the preference (attraction) of infected vectors for uninfected hosts:  $\alpha = 1$   
 97 means no preference,  $\alpha > 1$  preference and  $0 < \alpha < 1$  repulsion. Similarly, let  $u$  be  
 98 the preference of uninfected vectors for infected hosts. As in [9], only the spatial  
 99 movement of vectors is considered. Let  $D$  be the vector diffusion rate, independent  
 100 of the vector infection status. The model is:

$$\begin{aligned}
 I_t &= bpV \frac{\alpha(N-I)}{\alpha(N-I)+I} - rI, \\
 V_t &= bqU \frac{uI}{uI+(N-I)} - (m+l)V + DV_{xx}, \\
 U_t &= (m+l)V - bqU \frac{uI}{uI+(N-I)} + DU_{xx},
 \end{aligned} \tag{1}$$

101 in which the subscripts denote differentiation with respect to  $t$  or  $x$ , and in which the  
 102 dependence of the state variables on  $t$  and  $x$  has been omitted.

## 103 2.1 Model simplification

104 Let  $W = U + V$  be the total vector population density. We have  $W_t = DW_{xx}$ . Assuming  
 105  $W(x, 0) = K$  (the vector carrying capacity) for all  $x \in (-\infty, +\infty)$ ,  $W_t(x, 0) = 0$  for all  
 106  $x$ , meaning that  $W = K$  for all  $t \geq 0$  and  $x \in (-\infty, +\infty)$ . Therefore, we can substitute  
 107  $U$  with  $K - V$  in model (1), which thus simplifies to a two-dimensional system:

$$\begin{aligned}
 I_t &= bpV \frac{\alpha(N-I)}{\alpha(N-I)+I} - rI, \\
 V_t &= bq(K-V) \frac{uI}{uI+(N-I)} - (m+l)V + DV_{xx}.
 \end{aligned} \tag{2}$$

## 108 2.2 Non-dimensionalisation

109 We rescale the state variables and parameters by letting

$$\tau = (m+l)t, \quad \xi = x \sqrt{\frac{m+l}{D}}, \quad i = \frac{I}{N}, \quad v = \frac{V}{K}$$

110 and

$$\beta = \frac{bpK}{(m+l)N}, \quad \rho = \frac{r}{m+l}, \quad \theta = \frac{bq}{m+l}.$$

111 A dimensionless version of model (2) is the following:

$$\begin{aligned} i_\tau &= \beta v \frac{\alpha(1-i)}{\alpha(1-i)+i} - \rho i, \\ v_\tau &= \theta(1-v) \frac{ui}{ui+(1-i)} - v + v_{\xi\xi}, \end{aligned} \quad (3)$$

112 in which the subscripts denote differentiation with respect to  $\tau$  or  $\xi$ . Note that the  
113 two state variables are both disease prevalences, i.e. they are fractions of the host  
114 and the vector being infected, and take values in the unit interval.

### 115 **3 Analysis of the non-spatial system**

116 The non-spatial model is:

$$\begin{aligned} i' &= \beta v \frac{\alpha(1-i)}{\alpha(1-i)+i} - \rho i =: f_1(i, v), \\ v' &= \theta(1-v) \frac{ui}{ui+(1-i)} - v =: f_2(i, v). \end{aligned} \quad (4)$$

117 We will also use the following notations:  $y = (i, v)^T$  and  $f = (f_1, f_2)^T$ .

#### 118 **3.1 Basic reproductive number**

119 System (4) was previously explored in [47] and [14]. It is known that the disease-free  
120 equilibrium  $(i, v) = (0, 0)$  is locally asymptotically stable if and only if

$$\mathcal{R}_0^2 := \frac{b^2 pq K}{rm N} u = \frac{\beta \theta}{\rho} u < 1.$$

121 We refer to  $\mathcal{R}_0^2$  as the basic reproductive number. Note that  $\mathcal{R}_0$  depends on  $u$  (the  
122 preference of uninfected vectors for infected hosts) but does not depend on  $\alpha$  (the  
123 preference of infected vectors for uninfected hosts). The results we present next are  
124 original. Let  $u_c$  be such that  $\mathcal{R}_0^2 = 1$ , i.e.,

$$u_c = \frac{\rho}{\beta \theta}.$$

## 126 3.2 The system is cooperative

127 We have

$$\frac{\partial f_1}{\partial v} \geq 0 \quad \text{and} \quad \frac{\partial f_2}{\partial i} \geq 0,$$

128 since

$$\frac{\partial}{\partial i} \left( \frac{ui}{ui + (1-i)} \right) = \frac{u}{(1 + i(u-1))^2} > 0.$$

129 Therefore, system (4) is cooperative, meaning that the dynamics necessarily con-  
130 verge to an equilibrium (convergence to a limit cycle is impossible) [51].

## 131 3.3 Endemic equilibrium

132 Let us solve the system  $f_1(i, v) = f_2(i, v) = 0$ . An endemic equilibrium  $(i^*, v^*)$ , with  
133  $i^*, v^* > 0$ , satisfies:

$$Q(i^*) = Ai^{*2} + Bi^* + C = 0,$$

134 in which

$$\begin{aligned} A &= (a-1)(u(1+\theta)-1), \\ B &= \left( (2-(1+\theta)u) - \frac{\beta\theta}{\rho}u \right) a - 1 = -\left( ((1+\theta)u-1) + (\mathcal{R}_0^2-1) \right) a - 1, \\ C &= a \left( \frac{\beta\theta}{\rho}u - 1 \right) = a(\mathcal{R}_0^2 - 1). \end{aligned}$$

135 Let  $u^*$  be such that  $A = 0$ :

$$u^* = \frac{1}{1+\theta}. \quad (5)$$

136 Note that  $A$  has no reason to be zero in general ( $A = 0$  only for  $a = 1$  or  $u = u^*$ ). The  
137 coefficient  $A$  can be also expressed as

$$A = (a-1) \left( \frac{u}{u^*} - 1 \right).$$

138 First, we notice that

$$Q(1) = -u(1+\theta) < 0. \quad (6)$$

139 Next, we distinguish two cases:  $\mathcal{R}_0^2 > 1$  and  $\mathcal{R}_0^2 < 1$ . (The boundary case  $\mathcal{R}_0^2 = 1$  is  
 140 addressed in Appendix A.1 for the sake of completeness.)

### 141 **3.4 Case $\mathcal{R}_0^2 > 1$**

142 If  $\mathcal{R}_0^2 > 1$ , then  $Q(0) = C > 0$ . Since  $Q(1) < 0$  (Eq. 6), there is exactly one root  $i^*$  in  
 143  $[0, 1]$ , which is the endemic equilibrium. Appendix A.2 shows that

$$i^* = \begin{cases} -\frac{C}{B} & \text{if } \alpha = 1 \text{ or } u = u^* \text{ (special cases implying } A = 0), \\ \frac{1}{2A}(-B - \sqrt{\Delta}) & \text{otherwise,} \end{cases}$$

144 where  $\Delta = B^2 - 4AC$  is the discriminant.

### 145 **3.5 Case $\mathcal{R}_0^2 < 1$**

146 If  $\mathcal{R}_0^2 < 1$ , then  $C < 0$ .

147 Since  $Q(0) = C < 0$ , and  $Q(1) < 0$  (Eq. 6), either there is no root in between  
 148 0 and 1 or there are two roots (unless the discriminant  $\Delta$  is zero, in which case  
 149 there is a single root, of course). The existence of biologically feasible equilibria  
 150 requires  $A < 0$ . Since this implies  $AC > 0$ , an additional necessary condition for  
 151 the existence of endemic equilibria is that the discriminant  $\Delta$  is non-negative. The  
 152 additional conditions are  $Q'(0) = B > 0$  and  $Q'(1) = 2A + B < 0$ .

153 If these conditions ( $\mathcal{R}_0^2 < 1$ ,  $A < 0$ ,  $\Delta \geq 0$ ,  $B > 0$ , and  $2A + B < 0$ ) are simultaneously  
 154 satisfied, there are two positive equilibria with components

$$i_{1,2}^* = \frac{1}{2A}(-B \pm \sqrt{\Delta}), \quad (7)$$

155 since  $A < 0$  and  $B > 0$ . We set  $E_1 = (i_1^*, v_1^*)$  and  $E_2 = (i_2^*, v_2^*)$  and notice that the  
 156 equilibria are ordered, i.e.  $E_1 < E_2$ , since  $i_1^* < i_2^*$  and  $v_1^* = g(i_1^*) < v_2^* = g(i_2^*)$ , where  
 157  $g(i) = \frac{\rho}{\beta} \left(1 + \frac{i}{\alpha(1-i)}\right) i$  is an increasing function corresponding to  $f_1 = 0$  in (4).

#### 158 **3.5.1 Necessary conditions for two equilibria**

159 Here, we will derive two necessary conditions on the vector preferences, namely  
 160  $\alpha > 1$  and  $u < u^* < 1$  (since  $u^* = 1/(1 + \theta)$ , as defined in Eq. (5)), for two positive

161 equilibria to coexist.

162 First,  $B$  can be expressed as

$$B = -\left(1 + \theta + \frac{\theta\beta}{\rho}\right)au + (2a - 1).$$

163 Therefore,  $B > 0$  is equivalent to

$$u < \frac{(2a - 1)}{\left(1 + \theta + \frac{\theta\beta}{\rho}\right)a} =: u^+.$$

164 Second,  $B + 2A < 0$  can be expressed as

$$\left((\theta + 1)(a - 2) - \frac{\theta\beta}{\rho}a\right)u + 1 < 0. \quad (8)$$

165 A necessary condition for the inequality (8) to hold is

$$\frac{\theta\beta}{\rho(\theta + 1)} > \frac{a - 2}{a} =: R_1. \quad (9)$$

166 Assuming inequality (9) holds,  $B + 2A < 0$  (inequality 8) is equivalent to

$$u > \frac{1}{\frac{\theta\beta}{\rho}a - (\theta + 1)(a - 2)} =: u^-.$$

167 So far, we have shown that conditions  $B > 0$  and  $B + 2A < 0$  are equivalent to  $u < u^+$   
168 and  $u > u^-$  (provided inequality 8 holds), respectively. A necessary condition for  
169 these conditions to hold is therefore  $u^- < u^+$ . The latter inequality can be equiva-  
170 lently expressed as

$$\frac{1}{\frac{\theta\beta}{\rho}a - (\theta + 1)(a - 2)} < \frac{2a - 1}{\left(\left(1 + \frac{\beta}{\rho}\right)\theta + 1\right)a},$$

171 which is equivalent to

$$\left(1 + \frac{\beta}{\rho}\right)\theta + 1 < \left(2 - \frac{1}{a}\right)\left(\frac{\theta\beta}{\rho}a - (\theta + 1)(a - 2)\right).$$



172 After rearrangement, the above inequality can be equivalently expressed as

$$(\theta + 1)(a - 1)^2 < a(a - 1)\frac{\theta\beta}{\rho}.$$

173 A necessary condition for the above inequality to hold is  $a > 1$ . Assuming  $a > 1$ , this  
174 inequality can be equivalently expressed as

$$\frac{\theta\beta}{\rho(1 + \theta)} > \frac{a - 1}{a} =: R_2.$$

175 Since  $R_2 > R_1$ , the above inequality guarantees that inequality (9) is satisfied.

176 We were not able to get more results from this preliminary analysis, but we have  
177 shown that  $a > 1$  is a necessary condition for two endemic equilibria to coexist.

178 Assuming  $a > 1$ , the condition  $A < 0$  is equivalent to

$$u < \frac{1}{1 + \theta} = u^*.$$

179 Hence,  $a > 1$  and  $u < u^* < 1$  are necessary conditions for two positive equilibria to  
180 coexist.

### 181 3.5.2 Numerical example of bistability

182 Since necessary and sufficient conditions were hardly expressible with pen and pa-  
183 per, we used symbolic calculation software (Maple 2022) to disentangle the condi-  
184 tions for two positive equilibria to coexist. To simplify things, we let

$$X = u(1 + \theta) - 1 \quad \text{and} \quad Y = \mathcal{R}_0^2 - 1. \quad (10)$$

185 This way,

$$A = (a - 1)X, \quad B = -(X + Y)a - 1 \quad \text{and} \quad C = aY.$$

186 Since  $\mathcal{R}_0^2 < 1$ ,  $Y < 0$ . Since  $a > 0$ ,  $C < 0$ . The previous section showed that  $A < 0$ ,  
187  $a > 1$ , and therefore  $X < 0$  are necessary conditions for two positive equilibria to  
188 coexist. We thus used the function “solve” in Maple to solve the following system of

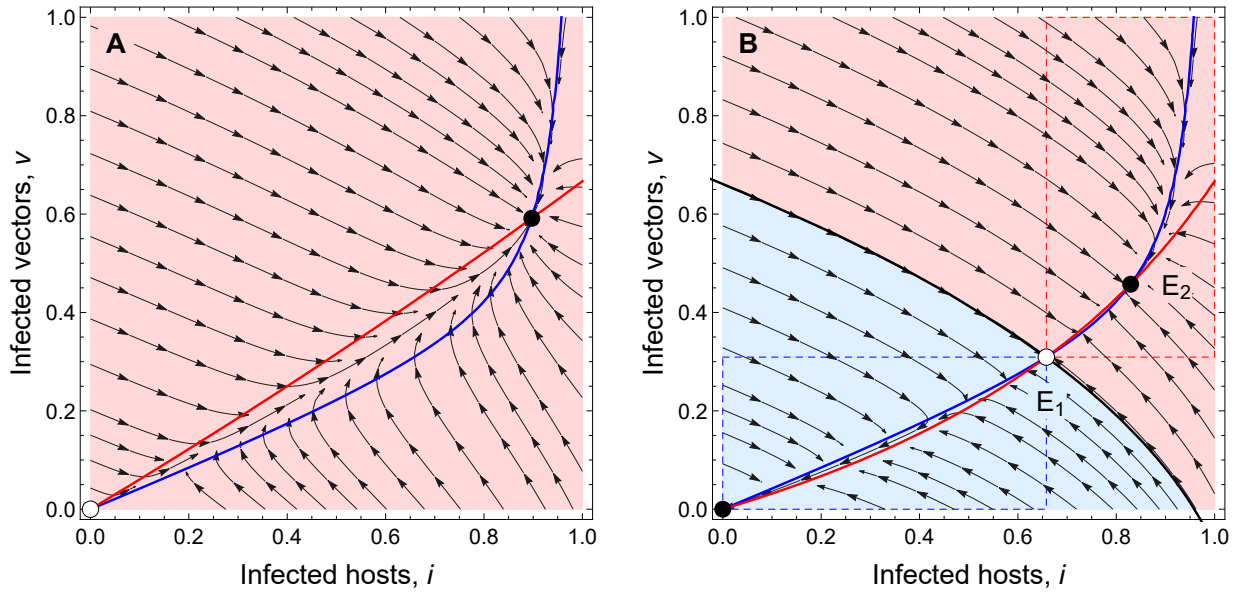


Figure 1: Phase portraits of the non-spatial model (4) with  $v$ - and  $i$ -nullclines (blue and red curves, respectively). Stable (unstable) equilibria are shown as filled (empty) circles. The basins of attraction to the endemic (disease-free) equilibrium are shown in light red (light blue). **(A)** The endemic equilibrium is the only attractor. Parameter value:  $u = 0.3$ , so  $\mathcal{R}_0^2 = 1.44 > 1$ . **(B)** Bistable case. The black line is the separatrix of the two basins of attraction. The dashed rectangles indicate analytically obtained sets of initial conditions that are known to approach the disease-free (blue) or endemic (red) equilibrium. They are part of the actual basins of attraction, see Sect. 3.6 for more details. Parameter value:  $u = 0.15$ , so  $\mathcal{R}_0^2 = 0.72 < 1$ . All other parameter values:  $a = 15, \beta = 2.4, \rho = 1, \theta = 2$ .

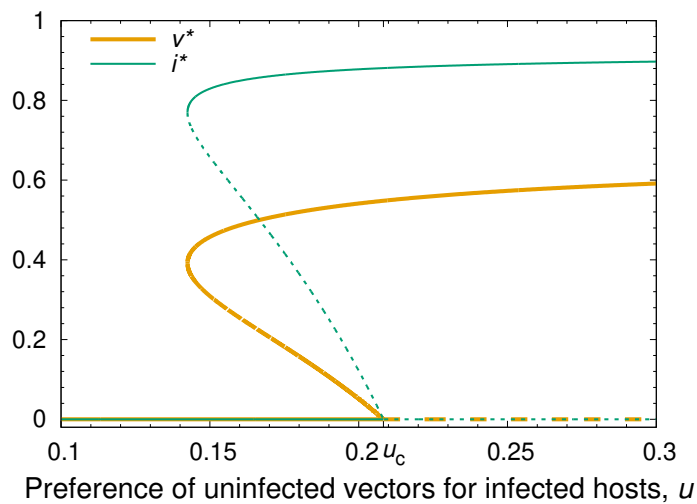


Figure 2: Bifurcation diagram of the non-spatial model (4). Stable (unstable) steady states are shown in solid (dashed) line. There is a backward bifurcation at  $u = u_c \approx 0.2083$  and a fold bifurcation at  $u \approx 0.1425$ . Other parameter values as in Fig. 1.

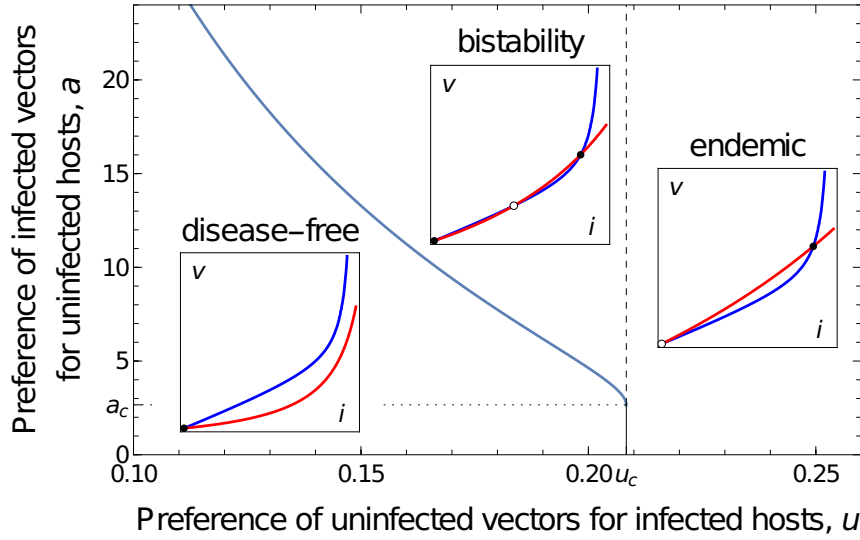


Figure 3: Two-parameter bifurcation diagram of the non-spatial model (4). The fold bifurcation where two endemic equilibria coalesce is shown in blue. The vertical line marks the transcritical bifurcation curve, which occurs at  $\mathcal{R}_0^2 = 1$ . When the vertical line is solid (dashed), there is a standard transcritical (backward) bifurcation. The fold and transcritical bifurcation curves meet at  $(u_c \approx 0.2083, a_c \approx 2.6666)$ . The insets are nullcline examples of parameter values leading to different dynamical regimes. Other parameter values as in Fig. 1.

189 inequalities,

$$A < 0, \quad B > 0, \quad (2A + B) < 0, \quad B^2 - 4AC > 0, \quad Y < 0, \quad a > 1, \quad X < 0$$

190 with respect to  $X, Y$  and  $a$ . Letting

$$h(Y, a) := \frac{Ya^2 - (2Y + 1)a - 2\sqrt{-Ya^2(a-1)(Y+1)}}{a^2},$$

191 we obtained the following set of conditions:

192 • If  $1 < a < 2$ ,

$$\frac{Ya + 1}{a - 2} < X < h(Y, a), \quad \text{and} \quad Y > -\frac{a - 1}{a}.$$

193 • If  $a = 2$ ,

$$X < -\frac{1}{2} - \sqrt{-Y(Y-1)} = h(Y, 2), \quad \text{and} \quad Y > -\frac{1}{2}.$$

- If  $a > 2$ :

$$\begin{cases} X < h(Y, a) & \text{if } Y > -\frac{1}{a}, \\ X < -4\frac{a-1}{a^2} = h\left(\frac{1}{a}, a\right) & \text{if } Y = -\frac{1}{a}, \\ \text{impossible} & \text{if } Y \in \left[-\frac{a-1}{a}, -\frac{1}{a}\right), \\ X < \frac{Ya+1}{a-2} & \text{if } Y < -\frac{a-1}{a}. \end{cases}$$

194 This condition set allowed us to find parameter values for which bistability occurs;  
 195 see Figs. 1–3 for phase portraits, one-parameter, and two-parameter bifurcation di-  
 196 agrams, respectively.

### 197 3.6 Local and global asymptotic stability

198 The system being monotone cooperative, proving global asymptotic stability (GAS)  
 199 relies on local asymptotic stability (LAS) and the use of some appropriate theorems.

The Jacobian of system (4) is

$$J(i, v) = \begin{pmatrix} -\beta v \frac{a}{(a(1-i)+i)^2} - \rho & \beta \frac{a(1-i)}{a(1-i)+i} \\ \theta(1-v) \frac{u}{(ui+(1-i))^2} & -\theta \frac{ui}{ui+(1-i)} - 1 \end{pmatrix}.$$

Notice that  $J(i, v)$  is irreducible for all  $(i, v) \in [0, 1]^2$ . At equilibrium  $(0, 0)$ , we have

$$J(0, 0) = \begin{pmatrix} -\rho & \beta \\ \theta u & -1 \end{pmatrix},$$

200 from which we deduce that  $0 = (0, 0)^T$  is LAS when  $\mathcal{R}_0^2 = \beta\theta u/\rho < 1$  and unstable  
 201 when  $\mathcal{R}_0^2 > 1$ .

202 When  $\mathcal{R}_0^2 > 1$ , only one positive endemic equilibrium,  $E$ , exists in  $[0, 1]^2$ . Thus,  
 203 when  $\mathcal{R}_0^2 > 1$ , using Theorem 6 in [1] [51], with  $\mathbf{a} = (0, 0)$  and  $\mathbf{b} = (1, 1)$  such  
 204 that  $f(\mathbf{b}) \leq 0 \leq f(\mathbf{a})$ , we deduce that the endemic equilibrium  $E$  is GAS on  $[0, 1]^2$ .  
 205 Similarly, when  $\mathcal{R}_0^2 < 1$ , in the case when no endemic equilibrium exists, we can  
 206 show, using the same approach, that  $0$  is GAS.

207 Assume  $\mathcal{R}_0^2 < 1$ . In the case where  $0$ ,  $E_1$ , and  $E_2$  co-exist such that  $0 \ll E_1 \ll$   
 208  $E_2$ , we already know that  $0$  is LAS. We can check (at least numerically) that  $E_1$  is

209 unstable and  $E_2$  is LAS. Following [51, Theorem 2.2.2], it is straightforward to show  
 210 that the set  $\{y \in \mathbb{R}^2 : 0 \leq y < E_1\}$  is in the basin of attraction of 0, while the set  
 211  $\{y \in \mathbb{R}^2 : E_1 < y \leq 1\}$ , where  $1 = (1, 1)^T$ , is in the basin of attraction of  $E_2$  (Fig. 1B).

## 212 **4 Back to the system with diffusion**

213 In this section, we get back to the system with diffusion, i.e., system (3).

### 214 **4.1 Existence and uniqueness of a solution**

System (3), with non-negative initial conditions and appropriate boundary conditions, is a partly dissipative or a partially degenerate system. We consider the following spaces

$$\mathcal{S} = \{(i, v) | v \in L^2(\mathbb{R}); i \in L^\infty(\mathbb{R})\},$$

and

$$\mathcal{S}_{1,1} = \{(i, v) \in \mathcal{S} | 0 \leq v \leq 1; 0 \leq i \leq 1\}.$$

215 Following **(author?)** [48, Theorem 1, page 111], or [45, Theorem 2.1], we can show  
 216 local existence and uniqueness. Then, using a priori  $L^\infty$  estimates, the fact that the  
 217 right-hand side of (3) is quasi-positive and the maximum principle lead to

**Theorem 1** (Existence and uniqueness). *For any initial values  $(i_0, v_0) \in \mathcal{S}_{1,1}$ , system (3) admits a unique non-negative bounded solution such that*

$$i \in C([0, \infty); L^\infty(\mathbb{R})) \cap C^1([0, \infty); L^\infty(\mathbb{R}))$$

and

$$v \in C([0, \infty); L^\infty(\mathbb{R})) \cap C([0, \infty); H^2(\mathbb{R})) \cap C^1([0, \infty); L^2(\mathbb{R})).$$

218 Since the study of the non-spatial system showed us that, depending on parameter  
 219 values, it can be monostable or bistable, it seems relevant to study the existence  
 220 (or non-existence) of travelling wave solutions.

## 221 4.2 Monostable case

222 In this section, we assume  $\mathcal{R}_0^2 > 1$ . We know from the non-spatial system that the  
223 disease-free equilibrium 0 is unstable and the endemic equilibrium  $E$  is GAS. Does a  
224 travelling wave solution connecting 0 to  $E$  exist?

### 225 4.2.1 Existence of a travelling wave

226 In the monostable case, the existence of a travelling wave should derive from the  
227 fact that the system is cooperative [40]; the problem is that the system is partially  
228 degenerate [18, 39]. However, for this situation powerful theorems exist [19, 39],  
229 see also [15].

Here, we will use Theorem 4.2 in [39] for the following system:

$$\frac{\partial \mathbf{y}}{\partial t} = D \frac{\partial^2 \mathbf{y}}{\partial x^2} + \mathbf{f}(\mathbf{y}(t, x)),$$

230 with  $\mathbf{y} = (y_1(t, x), \dots, y_k(t, x))$ ,  $D = \text{diag}(d_1, \dots, d_k) \geq 0$  and  $\mathbf{f} = (f_1, \dots, f_k)$ . According  
231 to [39], the following hypotheses have to be checked [Hypotheses 2.1 in 39]:

- 232 1. There is a proper subset  $\Sigma_0$  of  $\{1, \dots, k\}$  such that  $d_i = 0$  for  $i \in \Sigma_0$  and  $d_i > 0$   
233 for  $i \notin \Sigma_0$ .
- 234 2.  $\mathbf{f}(0) = 0$ , there is a constant  $\gamma \gg 0$  such that  $\mathbf{f}(\gamma) = 0$  which is minimal in the  
235 sense that there is no constant  $\nu$  other than  $\gamma$  such that  $\mathbf{f}(\nu) = 0$  and  $0 \ll \nu \ll \gamma$ ,  
236 and the equation  $\mathbf{f}(\alpha) = 0$  has a finite number of constant roots.
- 237 3. The system is cooperative.
- 238 4.  $\mathbf{f}(\alpha)$  is uniformly Lipschitz in  $\alpha$  such that there is  $\eta > 0$  such that for any  $\alpha_i$ ,  
239  $i = 1, 2$ ,  $\|(\alpha_1) - \mathbf{f}(\alpha_2)\| \leq \eta \|\alpha_1 - \alpha_2\|$ .
- 240 5.  $\mathbf{f}$  has the Jacobian  $\mathbf{f}'(0)$  at 0 with the property that  $\mathbf{f}'(0)$  has a positive eigen-  
241 value whose eigenvector has positive components.

Assuming  $\mathcal{R}_0^2 > 1$ , and  $k = 2$ , it is straightforward to check the first three hypotheses  
for system (3), where  $\gamma = E$ . The fourth hypothesis requires long computations for

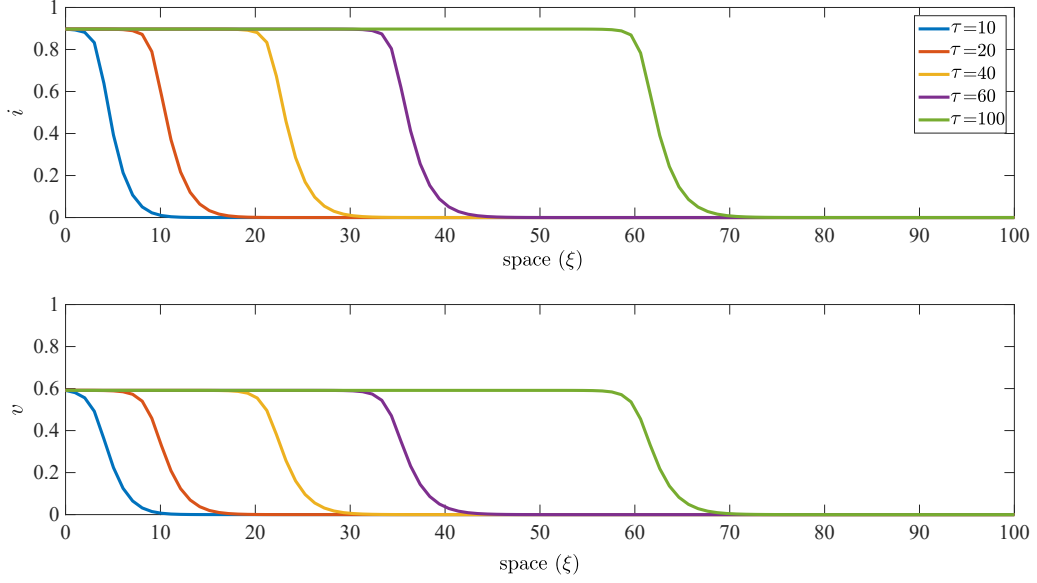


Figure 4: Monostable travelling wave solution of model (3) connecting the disease-free and endemic equilibria 0 and  $E$  when  $\mathcal{R}_0^2 = 1.44 > 1$ . Here  $u = 0.3$ , other parameter values as in Fig. 1.

$\alpha \neq 1$  and  $u \neq 1$  to be checked. Lastly, we have

$$\mathbf{f}'(0) = \begin{pmatrix} -\rho & \beta \\ \theta u & -1 \end{pmatrix}.$$

242 Since  $\mathcal{R}_0^2 > 1$ , it is straightforward to show that  $\mathbf{f}'(0)$  has a positive eigenvalue,  
 243  $\lambda = \frac{1}{2} \left( \sqrt{(1-\rho)^2 + 4\rho\mathcal{R}_0^2} - (1+\rho) \right)$ , associated with the positive eigenvector  $\left( 1, \frac{\lambda + \rho}{\beta} \right)^T$ .  
 244 Thus, according to Theorem 4.2 in [39], we deduce the existence of a travelling wave  
 245 connecting 0 to  $\gamma = E$ . See, for instance, Fig. 4.

#### 246 4.2.2 Derivation of the linear spreading speed

247 Still assuming  $\mathcal{R}_0^2 > 1$ , we consider a travelling front connecting the disease-free  
 248 equilibrium, 0 to the endemic equilibrium,  $E$ . We posit that, in some circumstances,  
 249 the front speed is linearly determined by the minimum possible wave speed based  
 250 on the linearisation at the leading edge of the wave. We apply the minimum wave  
 251 speed approach [36, 24, 3, 28, 25] to the linearised model to find the linear spreading  
 252 speed as a critical point. However, we stress that the linear spreading speed may  
 253 be only a lower bound of the actual spreading speed in some cases (see Fig. 11 in  
 254 Appendix B.2).

255 At the leading edge of the front invading the disease-free equilibrium,  $i$  and  $v$   
 256 have small positive values. We linearise system (3) at the leading edge:

$$\begin{aligned} i_\tau &= \beta v - \rho i, \\ v_\tau &= \theta u i - v + v_{\xi\xi}. \end{aligned}$$

257 We are interested in travelling wave solutions such that

$$y = \begin{pmatrix} i \\ v \end{pmatrix} = k \exp(-s(\xi - c\tau)),$$

258 in which  $k$  is an implicit column vector,  $c$  is the linear wave speed, and  $s$  is the  
 259 exponential decay rate of the wave profile at leading edge.

260 Plugging the previous expression in the system, we obtain

$$scy = \underbrace{\begin{bmatrix} -\rho & \beta \\ \theta u & -1 + s^2 \end{bmatrix}}_{M_s} y, \quad (11)$$

261 which implies that

$$\det \underbrace{\begin{bmatrix} -\rho - sc & \beta \\ \theta u & -1 + s^2 - sc \end{bmatrix}}_{M_s - sc\mathbb{I}} = 0,$$

262 in which  $\mathbb{I}$  is the identity matrix. This yields

$$\begin{aligned} 0 &= (-\rho - sc)(-1 + s^2 - sc) - \theta u \beta, \\ &= Fc^2 + Gc + H, \end{aligned} \quad (12)$$

263 with

$$F = s^2, \quad G = s(\rho + 1 - s^2), \quad H = \rho(1 - s^2) - \theta u \beta.$$

264 Next, we follow the approach of using Eq. (12) to calculate the minimum linear wave  
 265 speed as outlined in [24].



266 The discriminant of the quadratic in Eq. (12) is

$$\begin{aligned}\Lambda &= G^2 - 4FH, \\ &= s^2 \left( (\rho + 1 - s^2)^2 - 4\rho(1 - s^2) + 4\theta u\beta \right), \\ &= s^2 \left( (\rho - 1 + s^2)^2 + 4\theta u\beta \right) > 0.\end{aligned}$$

267 Since  $\Lambda > 0$ , there are two real roots:

$$z = \frac{-G - \sqrt{\Lambda}}{2F} \quad \text{and} \quad c = \frac{-G + \sqrt{\Lambda}}{2F}.$$

268 First, we show that  $z < 0$ . If  $G > 0$ , then  $z < 0$  since  $F > 0$ . Otherwise (if  $G < 0$ ),  
269 then  $-G - \sqrt{\Lambda} > 0$  is equivalent to  $0 > -4FH$ , which is impossible since  $H < 0$  (this is  
270 because  $G < 0$  implies  $1 - s^2 < 0$ ).

271 Second, we show that  $c > 0$  for all  $s > 0$ . If  $G < 0$ , then  $c > 0$  since  $F > 0$ .  
272 Otherwise (if  $G > 0$ ), then  $-G + \sqrt{\Lambda} > 0 \Leftrightarrow \Lambda > G^2$  is equivalent to  $\mathcal{R}_0^2 > 1 - s^2$ , which  
273 is satisfied since we assume  $\mathcal{R}_0^2 > 1$  in this section.

274 The relevant root is therefore  $c$ . Since Eq. (12) only depends on three additional  
275 parameters,  $s$ ,  $\rho$  and  $\beta\theta u$ , we express  $c$  as a function of these parameters:

$$c(s, \rho, \beta\theta u) = \frac{-(\rho + 1 - s^2) + \sqrt{(\rho - 1 + s^2)^2 + 4\theta u\beta}}{2s}.$$

276 Since  $c$  is a convex function of  $s$  (Appendix B.1),  $\lim_{s \rightarrow 0} c(s, \rho, \beta\theta u) = +\infty$ , and  
277  $\lim_{s \rightarrow +\infty} c(s, \rho, \beta\theta u) = +\infty$ , there exists a minimum to  $c$  with respect to  $s > 0$ .

278 Equation (12) can also be written to include the dependency of  $c$  on  $s$ ,  $\rho$ , and  $\beta\theta u$   
279 as

$$P(c(s, \rho, \beta\theta u), s) := (-\rho - sc)(-1 + s^2 - sc) - \theta u\beta.$$

280 Differentiating with respect to  $s$ , we have, for all  $s$ ,

$$\frac{dP}{ds} = \frac{\partial P}{\partial c} \frac{\partial c}{\partial s} + \frac{\partial P}{\partial s} = 0. \quad (13)$$

281 We are interested in the minimum possible linear wave speed. Let

$$s^*(\rho, \beta\theta u) = \arg \min_s c(s, \rho, \beta\theta u),$$

282 and

$$c^*(\rho, \beta\theta u) = c(s^*(\rho, \beta\theta u), \rho, \beta\theta u).$$

283 Since  $c^*$  is such that  $\partial c/\partial s = 0$ , Eq. (13) yields

$$\frac{\partial P}{\partial s}(c^*(\rho, \beta\theta u), s^*(\rho, \beta\theta u)) = 0. \quad (14)$$

284 Since  $P$  is cubic in  $s$ ,  $\partial P/\partial s$  is quadratic in  $s$ . We are interested in the conditions  
 285 on the coefficients that allow both polynomials to have a common root,  $s^*$ . They are  
 286 given by cancelling the resultant of the two polynomials. Letting  $P = es^3 + fs^2 + gs + h$   
 287 yields  $\partial P/\partial s = 3es^2 + 2fs + g$ . The coefficients are identified as

$$e = -c, \quad f = c^2 - \rho, \quad g = (\rho + 1)c, \quad h = -\theta u\beta + \rho.$$

288 The resultant is  $r(e, f, g, h) = -e(f^2g^2 - 4eg^3 - 4f^3h + 18efgh - 27e^2h^2)$ , as described  
 289 in [32, Eq. (4.3)]. The equality  $r(e, f, g, h) = 0$  can be equivalently expressed as a  
 290 cubic with respect to  $c^2$ :

$$c_3(c^2)^3 + c_2(c^2)^2 + c_1(c^2)^1 + c_0 = 0, \quad (15)$$

291 with

$$\begin{aligned} c_3 &= 4\beta\theta u + (\rho - 1)^2, \\ c_2 &= 2\rho^3 + 2\rho^2 + (6\beta\theta u - 8)\rho + 18\theta u\beta + 4, \\ c_1 &= \rho^4 + 8\rho^3 - (6\beta\theta u + 8)\rho^2 + 36u\rho\beta\theta - 27u^2\beta^2\theta^2, \\ c_0 &= -4\rho^3(\beta\theta u - \rho) = -4\rho^4(\mathcal{R}_0^2 - 1). \end{aligned}$$

292 Since we assume  $R_0^2 > 1$ , we have that  $c_0$  is negative and  $c_3$  is positive, which  
 293 means that we are in the same configuration as [24]. This implies that  $c^*(\rho, \beta\theta u)$  is  
 294 uniquely defined as the square root of the largest root of the above cubic.

295 Although it is possible to write down the formula for the largest root of a cu-  
 296 bic polynomial, we have no simple expression of  $c^*(\rho, \beta\theta u)$ . Figure 5 shows the  
 297 minimum linear speed of the monostable travelling wave solution as a function of  $u$ ,  
 298 as obtained by solving the cubic equation (15).

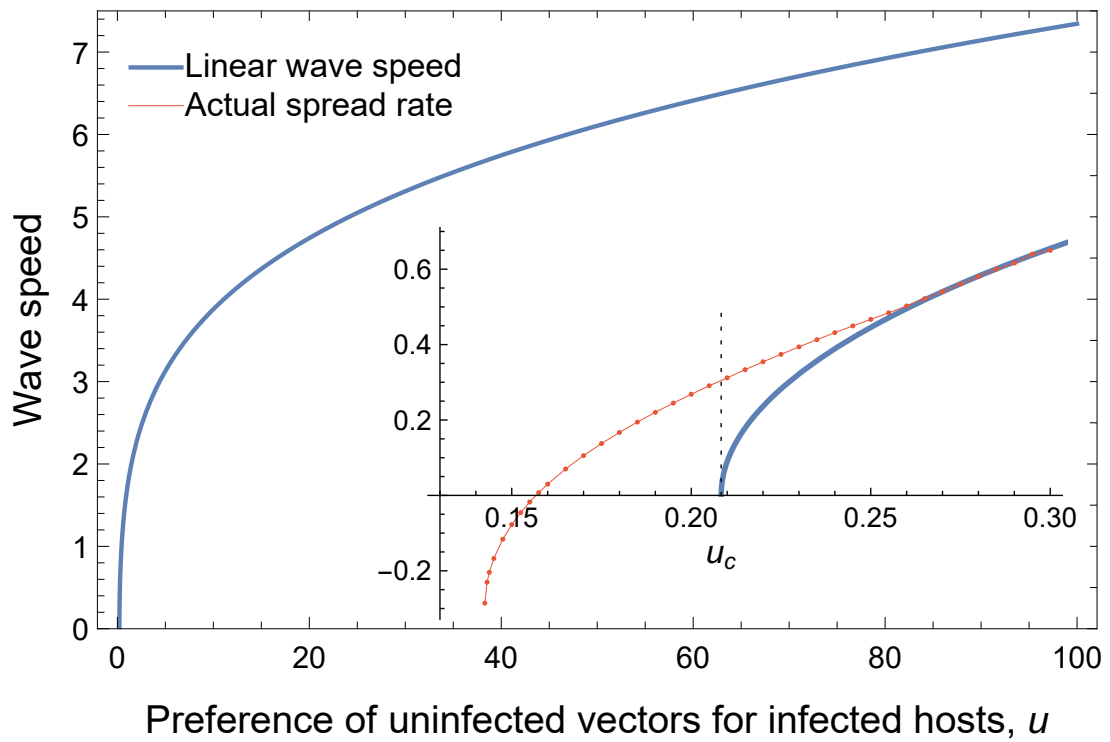


Figure 5: Linear speed of the monostable travelling wave as a function of  $u$  (the preference of uninfected vectors for infected hosts). The inset zooms on small values of  $u$  and compares the linear and actual (numerically computed) spreading speeds in model (3). The spreading speed is not linearly determined in the bistable case ( $u < u_c$ ) and in the monostable case ( $u > u_c$ ) for  $u$  close to  $u_c$ . However, the actual speed quickly converges to the linear speed as  $u$  increases. Other parameter values as in Fig. 1.

## 299 **4.3 Bistable case**

300 In this section, we assume  $\mathcal{R}_0^2 < 1$ .

### 301 **4.3.1 Existence of a travelling wave**

302 To show the existence of a bistable travelling wave solution, we will consider Theo-  
303 rem 4.2 in [18]. We have to verify that assumption (L):  $f \in C^1(\mathbb{R}^2, \mathbb{R}^2)$  satisfies the  
304 following conditions:

- 305 1.  $f(0) = f(E_2) = f(E_1) = 0$ , with  $0 \ll E_1 \ll E_2$ . There is no  $\eta$  other than 0,  $E_1$  and  $E_2$   
306 such that  $f(\eta) = 0$ , with  $0 \leq \eta \leq E_2$ .
- 307 2. System (3) is cooperative.
3.  $y \equiv 0$  and  $y \equiv E_2$  are stable while  $y \equiv E_1$  is unstable, that is

$$\lambda_0 := s(f'(0)) < 0, \quad \lambda_{E_2} := s(f'(E_2)) < 0, \quad \lambda_{E_1} = s(f'(E_1)) > 0.$$

- 308 4.  $f'(0)$ ,  $f'(E_1)$ , and  $f'(E_2)$  are irreducible.

309 Assuming that assumption (L) holds, then according to Theorem 4.2 in [18], sys-  
310 tem (3) admits a monotone wavefront  $(U, c)$  with  $U(-\infty) = 0$  and  $U(+\infty) = E_2$ .

311 Since  $\mathcal{R}_0^2 < 1$ , two positive endemic equilibria,  $E_1$  and  $E_2$ , exist. Equilibrium  $E_1$  is  
312 unstable while  $E_2$  is LAS. Thanks to the results obtained in Section 3, it is straight-  
313 forward to check that assumption (L) holds and to conclude that a travelling wave  
314 solution connecting 0 and  $E_2$  exists. See, for instance, Fig. 6.

315 In Fig. 7, we show that for  $u$  sufficiently small, the sign of the spreading speed  
316 can change. Thus, in the bistable case, for a given  $a \gg 1$ , there exist  $u^\dagger$  and  $u^{*,\dagger}$   
317 such that for  $u^\dagger < u < u^*$  the disease travelling wave moves forward, while for  
318  $u^{*,\dagger} < u < u^\dagger$  the disease travelling wave moves backward. When  $u < u^{*,\dagger}$  then the  
319 system converges to 0.

### 320 **4.3.2 Quasi-steady-state approximation**

321 For the case of a quasi-steady-state approximation (QSSA) (see Appendix B.2 for  
322 details), we can gain more information on the parameter domain for which the trav-

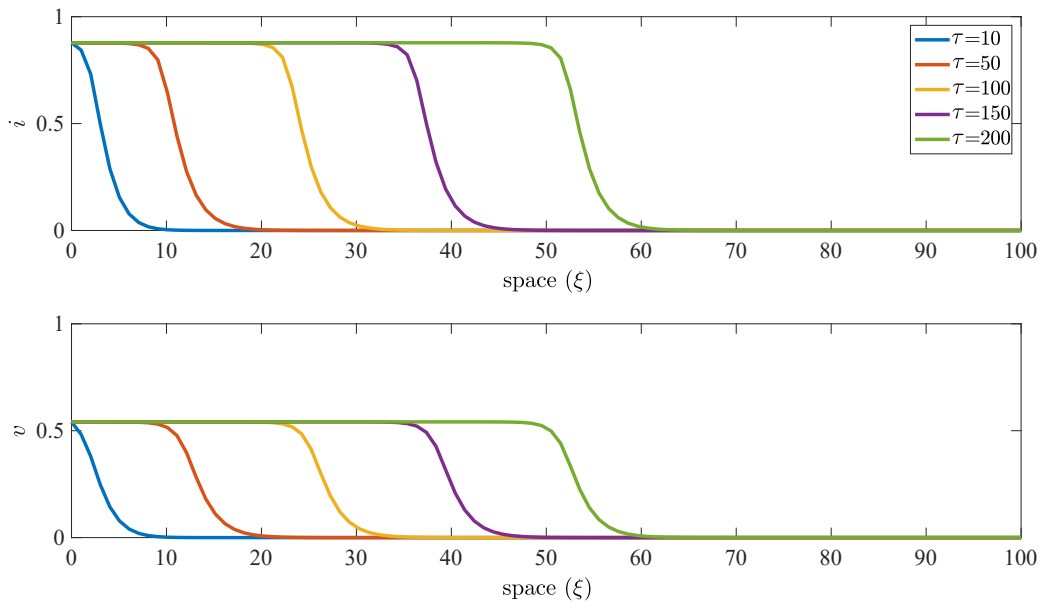


Figure 6: Bistable travelling wave solution of model (3) connecting the disease-free and endemic equilibria  $0$  and  $E_2$  when  $\mathcal{R}_0^2 = 0.96 < 1$ . Here  $u = 0.2$ , other parameter values as in Fig. 1. The disease is invading,  $c^* > 0$ .

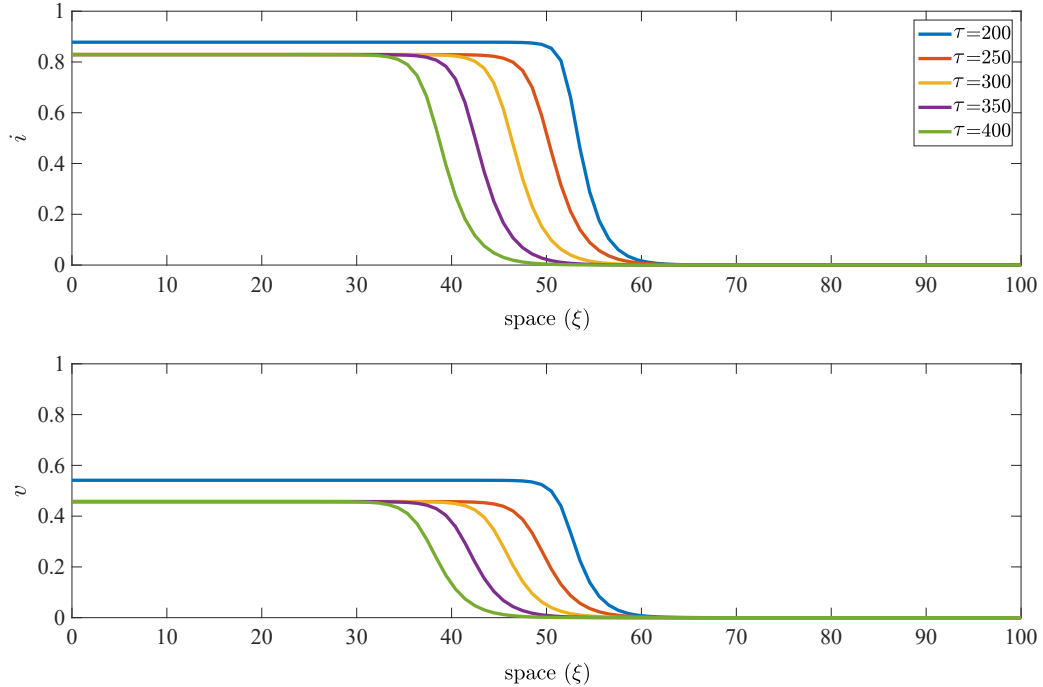


Figure 7: Bistable travelling wave solution of model (3) connecting the disease-free and endemic equilibria  $0$  and  $E_2$  when  $\mathcal{R}_0^2 = 0.72 < 1$ . Here  $u = 0.15$ , other parameter values as in Fig. 1. Starting at  $t = 200$  with the solution from Fig. 6 as initial condition, the spread is reversing,  $c^* < 0$ . This shows that a small variation of the parameter  $u$  (switching from  $u = 0.2$  in Fig. 6 to  $u = 0.15$  in this figure) can make the spreading speed switch from positive to negative. This is why the equilibrium prevalences decrease compared to initial conditions (at  $t = 200$ ).

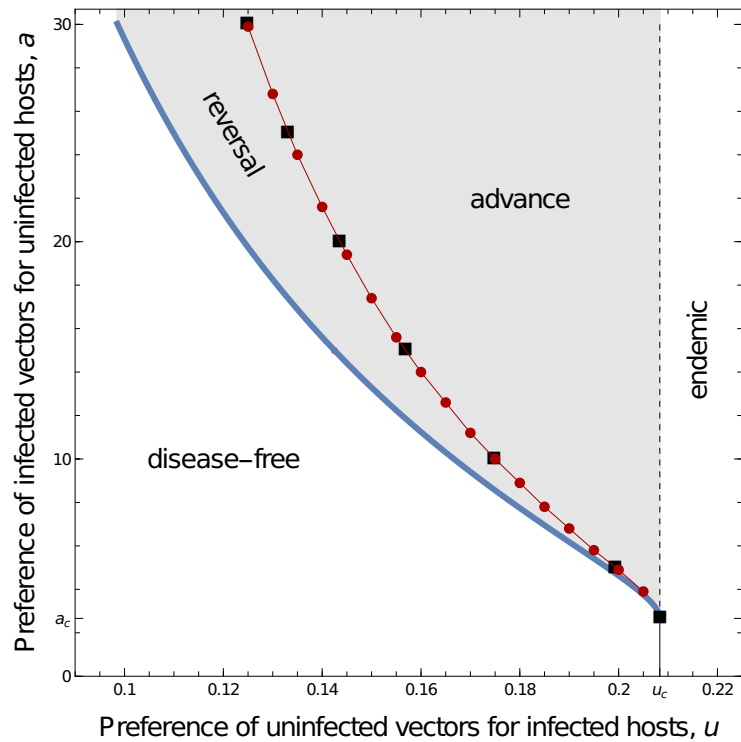


Figure 8: Within the bistable parameter domain (light grey), travelling waves connecting the disease-free and endemic equilibria can reverse or advance. The parameter domains of reversal and advance are separated by a curve corresponding to stalled waves with zero wave speed. Here, the zero-wave speed curve is obtained, on the one hand, by numerical integration of the PDE system (3) with  $\rho = 1$ ,  $\beta = 2.4$ ,  $\theta = 2$  and identifying parameter values to result in zero wave speed, accurate to at least the third decimal place (grey squares). On the other hand, the zero wave speed curve was indicated by Eq. (25) in Appendix B.2 using a quasi-steady-state assumption (red points). Other curves as in Fig. 3.

323 elling wave moves forward or backward. The direction is given by the expression (25)  
324 in Appendix B.2.

325 Figure 8 marks the boundary between wave advancement and reversal by red  
326 dots. This boundary corresponds to stalled traveling waves with speed zero. The  
327 QSSA results match very well with the zero wave speeds in the original system with-  
328 out a quasi-steady-state approximation (dark grey squares). This match may be  
329 particularly surprising because we have chosen a time scale parameter of  $\rho = 1$  for  
330 the simulations, while the QSSA is based on the assumption  $\rho \gg 1$ . However, Fig. 9  
331 in Appendix B.2 suggests that the wave speed approximations do not deviate much  
332 from the exact solutions for small spreading speeds and  $\rho \geq 1$ . This behaviour might  
333 explain why the QSSA correctly locates the  $c = 0$  curve in Fig. 8.

334 In the monostable case, the QSSA allows us to derive an explicit expression for  
335 the linear wave speed (see Eq. (23) in Appendix B.2), which is simply  $c^* = 2\sqrt{\mathcal{R}_0^2 - 1}$ .  
336 However, the linear spreading speed is only a lower bound of the actual spreading  
337 speed in some cases (Fig. 11).

## 338 5 Discussion

339 We have shown that conditional vector preferences may result in bistability between  
340 the disease-free equilibrium and an endemic equilibrium. The novelty compared to  
341 [22] and [14] is that bistability here occurs in the absence of any epidemiological  
342 feedback on vector population dynamics.

343 More specifically, we have shown that conditional vector preferences can cause a  
344 “backward bifurcation” (Fig. 2), meaning that  $\mathcal{R}_0^2 < 1$  is not a sufficient condition for  
345 the disease to go extinct [23].

### 346 5.1 Bistability conditions

347 We have shown that for bistability to occur, the following necessary conditions must  
348 be satisfied:  $\mathcal{R}_0^2 < 1$ ,  $a > 1$  and  $u < u^* < 1$ . The first condition ( $\mathcal{R}_0^2 < 1$ ) means that  
349 the basic reproductive number of the pathogen is not large enough for the pathogen  
350 to invade a disease-free population. Hence, the disease-free equilibrium is locally  
351 stable. However, if the prevalence of the infection is initially high, and if infected

352 vectors have a sufficiently strong preference for uninfected hosts ( $a > 1$ ), we have  
353 shown that the pathogen may persist in the population (an endemic equilibrium  
354 is locally stable as well) even though  $\mathcal{R}_0^2 < 1$ . These two conditions ( $a > 1$  and  
355  $\mathcal{R}_0^2 < 1$ ) are not too surprising. The third condition (implying  $u < 1$ ) is less intuitive.  
356 To interpret it, we recall that  $\mathcal{R}_0^2$  is proportional to  $u$ . If  $\mathcal{R}_0^2 < 1$  in spite of  $u > 1$   
357 (uninfected vectors prefer infected hosts, which is advantageous for the pathogen),  
358 this means that the pathogen has poor reproductive abilities. Therefore, even if  
359 the prevalence of the infection is initially high, the pathogen still goes extinct. By  
360 contrast, if  $\mathcal{R}_0^2 < 1$  while  $u < 1$  (uninfected vectors prefer uninfected hosts), it may  
361 be that the pathogen has strong enough reproductive abilities not to go extinct when  
362 its prevalence is initially high, and infected vectors prefer uninfected hosts ( $a > 1$ ).

## 363 **5.2 Travelling waves**

### 364 **5.2.1 Monostable case**

365 In the monostable case ( $\mathcal{R}_0^2 > 1$ ), the disease invades the spatial domain. We have  
366 shown that the linear spreading speed depends only on  $\rho$  and  $\beta\theta u$ , meaning that it  
367 does not depend on  $a$ , the preference of infected vectors for uninfected hosts. The  
368 interpretation is the same as for the basic reproductive number,  $\mathcal{R}_0^2 = \beta\theta u/\rho$ , which  
369 does not depend on  $a$  either [47, 22, 14]. In a situation close to the disease-free  
370 equilibrium, like at the leading edge of the front, there are so few infected hosts  
371 that the preference of infected vectors for uninfected hosts has a negligible effect  
372 on the dynamics. However, even in the monostable case, the spreading speed may  
373 not be linearly determined (Fig. 5), implying that it may depend on  $a$  (Fig. 12).  
374 This is due to the fact that disease spread is not driven by the leading edge of  
375 the invasion front (“pulled wave”). Instead, the disease invasion is driven by the  
376 whole of the front (“pushed wave”) [52, 38]. In particular, the disease spread may  
377 be maximum for intermediate prevalences because of the conditional preferences  
378 (similar to weak and strong Allee effects where population growth is strongest at  
379 intermediate densities). By contrast, dynamics of pulled waves are independent  
380 from the nonlinearities behind the leading edge of the front.



## 381 **5.2.2 Bistable case**

382 In the bistable case (requiring  $\mathcal{R}_0^2 < 1$ ), the disease either invades or retreats, de-  
383 pending on parameter values. More specifically, travelling waves may have negative  
384 speeds, meaning that the disease retreats.

385 In an epidemiological context, such a “front reversal” has been shown to occur  
386 when host population dynamics in the absence of disease are bistable, due, for  
387 instance, to a strong Allee effect in the host [29, 27]. However, to our knowledge,  
388 such a phenomenon has seldom [6] been shown to occur when bistability is due  
389 solely to the epidemiological dynamics.

## 390 **5.3 Biological implications**

391 Although conditional vector preferences might occur in human and animal diseases,  
392 they have so far been shown mainly in plant diseases [22]. Therefore, we now  
393 discuss plant diseases more specifically.

394 Plant diseases are a main threat to global food security [46]. Many plant dis-  
395 eases are caused by pathogens (viruses, bacteria and others) that are transmitted  
396 by insect vectors such as aphids, whiteflies, and others [16]. Infected vectors can  
397 be attracted to uninfected plants. This is for instance the case for aphids, *Rhopalosi-*  
398 *phum padi*, infected by the Barley yellow dwarf virus (BYDV) [31]. In his review of  
399 evidence for conditional vector preferences, [22] identified the volatile compounds  
400 emitted by infected plants as an attraction mechanism for (uninfected) vectors. For  
401 instance, plants infected by the *Cucumber mosaic virus* (CMV) or the *Tomato chloro-*  
402 *sis virus* (ToCV) produce volatiles that attract aphids or whiteflies [20]. Note also  
403 that vectors can be attracted to infected plants by visual cues, such as, for instance,  
404 yellow leaves.

405 Since the basic reproductive number of the pathogen ( $\mathcal{R}_0^2$ ) is proportional to  $u$   
406 (the preference of uninfected vectors for infected hosts), a plant variety that emits  
407 fewer volatiles could be considered resistant to disease. When visual cues are re-  
408 sponsible for vector preferences, a plant variety that expresses fewer symptoms,  
409 and is therefore less attractive to uninfected vectors, could also be considered resis-  
410 tant. Deployment of such resistant hosts might make it possible to obtain  $\mathcal{R}_0^2 < 1$ .  
411 We have shown that  $u \geq 1$  (a preference of uninfected vectors for infected hosts)

412 ensures disease extinction in this case ( $\mathcal{R}_0^2 < 1$ ), since bistability requires  $u < 1$ .  
413 This means that breeding for varieties that emit, when infected, a concentration  
414 of volatiles that is lower than that of standard varieties is a possible strategy for  
415 the control of vector-borne diseases (in combination with other strategies such as  
416 roguing - i.e., removing - infected plants, for instance).

#### 417 **5.4 Mathematical prospects**

418 An alternative for modelling vector preference could be density-dependent advec-  
419 tion (in analogy to preytaxis, this could perhaps be called “hosttaxis”). It has been  
420 shown that preytaxis in the presence of disease, where predators are attracted to  
421 or repelled by infected prey, can speed up or even lead to irregularly fluctuating  
422 travelling waves [4]. While [9] considered a “hosttaxis” term in their model, it was  
423 only a vector bias towards infected hosts, regardless of whether the vector carries  
424 the pathogen or not. Modelling conditional vector preferences with a hosttaxis term  
425 is beyond the scope of this paper and is left for future research.

426 **Acknowledgments:** FMHa and YD gratefully acknowledge partial funding from the  
427 MODCOV19 CNRS platform. FMHa’s visit in La Réunion (3P, Saint-Pierre) was partly  
428 supported by the European Agricultural Fund for Rural Development (EAFRD) within  
429 the DPP “Santé&Biodiversité” framework. YD is (partially) supported by the DST/NRF  
430 SARChI Chair in Mathematical Models and Methods in Biosciences and Bioengineer-  
431 ing at the University of Pretoria, South Africa (Grant 82770). YD acknowledges the  
432 support of the Conseil Régional de la Réunion (France), the Conseil Départemental de  
433 la Réunion (France), the European Agricultural Fund for Rural Development (EAFRD)  
434 and the Centre de Coopération Internationale en Recherche Agronomique pour le  
435 Développement (CIRAD), France. The authors thank the reviewers for their insightful  
436 comments and helpful suggestions.

437

#### 438 **A Side results on the non-spatial model**

439 **A.1 Case  $\mathcal{R}_0^2 = 1$  (boundary case)**

440 If  $\mathcal{R}_0^2 = 1$ , or equivalently

$$u = \frac{\rho}{\beta\theta},$$

then  $C = 0$  and  $i^* = -B/A$ . Using the above expression of  $u$  yields

$$i^* = 1 - \frac{1}{(a-1)\left(\frac{\beta\theta}{(1+\theta)\rho} - 1\right)}.$$

441 If  $a = 1$ , the endemic equilibrium does not exist. In what follows, we assume  $a \neq 1$ .

442 Let the fraction of susceptible hosts at equilibrium be

$$s^* = \frac{1}{(a-1)\left(\frac{\beta\theta}{(1+\theta)\rho} - 1\right)}.$$

443 We have:

$$s^* > 0 \Leftrightarrow \begin{cases} \frac{\beta\theta}{(1+\theta)\rho} > 1 & \text{if } a > 1, \\ \frac{\beta\theta}{(1+\theta)\rho} < 1 & \text{if } a < 1. \end{cases}$$

444 Assuming  $s^* > 0$ ,  $s^* < 1$  is equivalent to

$$(a-1)\left(\frac{\beta\theta}{(1+\theta)\rho} - 1\right) > 1.$$

445 Two cases can then be distinguished:

446 • If  $a > 1$ ,  $s^* < 1$  is equivalent to

$$\frac{\beta\theta}{(1+\theta)\rho} - 1 > \frac{1}{a-1} \Leftrightarrow \frac{\beta\theta}{(1+\theta)\rho} > \frac{a}{a-1}.$$

447 • If  $a < 1$ ,  $s^* < 1$  is equivalent to

$$\left(1 - \frac{\beta\theta}{(1+\theta)\rho}\right)(1-a) > 1 \Leftrightarrow 1 - \frac{\beta\theta}{(1+\theta)\rho} > \frac{1}{1-a} \Leftrightarrow -\frac{\beta\theta}{(1+\theta)\rho} > \frac{a}{1-a},$$

448 which is impossible.

449 Therefore,  $0 < s^* < 1$  if and only if

$$a > 1 \quad \text{and} \quad \frac{\beta\theta}{(1+\theta)\rho} > \frac{a}{a-1} > 1. \quad (16)$$

450 **A.2 Case  $\mathcal{R}_0^2 > 1$**

451 To derive the expression of the endemic equilibrium, we consider three cases:  $a = 1$ ,  
 452  $0 < a < 1$  and  $a > 1$ .

453 **Case  $a = 1$ .** If  $a = 1$ , then  $A = 0$  and

$$i^* = -\frac{C}{B}.$$

454 Since  $\mathcal{R}_0^2 > 1$ ,

$$B = -((1 + \theta)u + \mathcal{R}_0^2 - 1) < 0.$$

455 Therefore,

$$i^* = \frac{\mathcal{R}_0^2 - 1}{(1 + \theta)u + \mathcal{R}_0^2 - 1}.$$

456 We have  $0 < i^* < 1$ .

457 **Case  $0 \leq a < 1$ .** Since

$$B = -(((1 + \theta)u + \mathcal{R}_0^2 - 1)a + (1 - a)),$$

458 we deduce that  $B < 0$ . Then, we have three sub-cases to consider:

459 • If  $u > u^*$ , then  $A < 0$ . The relevant root is therefore the largest:

$$\frac{1}{2A}(-B - \sqrt{\Delta}),$$

460 since the other root is negative.

461 • If  $u = u^*$ ,  $A = 0$ . We obtain

$$i^* = \frac{\mathcal{R}_0^2 - 1}{\mathcal{R}_0^2 - 1 + \frac{1}{a}}. \quad (17)$$

462 We have  $0 < i^* < 1$ .

463 • If  $u < u^*$ , then  $A > 0$ . The relevant root is therefore the smallest:

$$\frac{1}{2A}(-B - \sqrt{\Delta}),$$

Table 1: The component  $i^*$  of the endemic equilibrium in the specific case  $\mathcal{R}_0^2 > 1$ , expressed as a function of  $A$ ,  $B$ ,  $C$  and  $\Delta = B^2 - 4AC$ .

	$0 < a < 1$	$a = 1$	$a > 1$
$u < u^*$	$\frac{1}{2A}(-B - \sqrt{\Delta})$	$-\frac{C}{B}$	$\frac{1}{2A}(-B - \sqrt{\Delta})$
$u = u^*$	$-\frac{C}{B}$	$-\frac{C}{B}$	$-\frac{C}{B}$
$u > u^*$	$\frac{1}{2A}(-B - \sqrt{\Delta})$	$-\frac{C}{B}$	$\frac{1}{2A}(-B - \sqrt{\Delta})$

464 since both roots are positive.

465 **Case  $a > 1$ .** We again distinguish three sub-cases:

466 • If  $u > u^*$ , then  $A > 0$  and  $B < 0$ . The relevant root is therefore the smallest:

$$\frac{1}{2A}(-B - \sqrt{\Delta}),$$

467 since both roots are positive.

468 • If  $u = u^*$ ,  $A = 0$ . We again find expression (17).

469 • If  $u < u^*$ , then  $A < 0$ . The relevant root is therefore the largest:

$$\frac{1}{2A}(-B - \sqrt{\Delta}),$$

470 since the other root is negative.

471 These results are summarized in Tab. 1.

472

### 473 **A.3 Case $\mathcal{R}_0^2 < 1$**

474 We here focus on the necessary condition  $\Delta = B^2 - AC > 0$  for the existence of

475 two endemic equilibria in the case  $\mathcal{R}_0^2 < 1$ . Using the notations  $X = u(1 + \theta) - 1$  and

476  $Y = \mathcal{R}_0^2 - 1$  (Eq. (10)) yields the following expression of  $\Delta$  as a quadratic function of

477  $a$ :

$$\Delta = (X - Y)^2 a^2 + 2(X(1 + Y) + Y(1 + X))a + 1.$$

478 Since  $(X - Y)^2 > 0$ , this parabola has a U-shape. We also have  $\Delta(0) = 1 > 0$ . There-

479 fore, either there are two positive roots,  $a_c^-$  and  $a_c^+$ , or there are none. In the latter

480 case,  $\Delta > 0$  regardless of the value of  $a$ . In case there are two roots, the largest one,

$$a_c^+ = \frac{-((X(1+Y) + Y(1+X)) + 2\sqrt{XY(1+X)(1+Y)})}{(X-Y)^2},$$

481 can also be expressed as

$$a_c^+ = \left( \frac{\sqrt{-X(1+Y)} + \sqrt{-Y(1+X)}}{X-Y} \right)^2.$$

482 Similarly,  $a_c^-$  can be expressed as

$$a_c^- = \left( \frac{\sqrt{-X(1+Y)} - \sqrt{-Y(1+X)}}{X-Y} \right)^2.$$

483 Since  $1+X = u(1+\theta) > 0$ ,  $1+Y = \mathcal{R}_0^2 > 0$ , and  $Y = \mathcal{R}_0^2 - 1 < 0$ , the existence of two  
484 conjugate roots requires  $X = u(1+\theta) - 1 < 0$ , or equivalently  $u < u^*$ .

485 We now focus on the condition  $a > a_c^+$  (implying  $\Delta > 0$ ) since it happens to co-  
486 incide with the separatrix we numerically obtained in the parameter space (Fig. 3).

487 Let us express  $a_c^+$  as a function of the original parameters:

$$a_c^+ = \left( \frac{\sqrt{-(u(1+\theta)-1)\mathcal{R}_0^2} + \sqrt{-(\mathcal{R}_0^2-1)u(1+\theta)}}{u(1+\theta) - \mathcal{R}_0^2} \right)^2, \quad (18)$$

488 or equivalently:

$$a_c^+(u) := \left( \frac{\sqrt{(1-\frac{u}{u^*})\mathcal{R}_0^2} + \sqrt{(1-\mathcal{R}_0^2)\frac{u}{u^*}}}{\frac{\mathcal{R}_0^2}{u^*}(u_c - u^*)} \right)^2.$$

489 Assuming  $a_c^+(u)$  is defined for all  $u \in [0, u_c]$  implies  $u_c < u^*$ .

490 In particular, since  $u_c$  is such that  $\mathcal{R}_0^2 = 1$ , we have

$$a_c^+(u_c) = \frac{1}{1 - \frac{u_c}{u^*}} =: a_c. \quad (19)$$

491 The condition  $a > a_c$  (implying  $a > 1$ ) is equivalent to the condition we obtained for  
492 the existence of an endemic equilibrium in the boundary case  $\mathcal{R}_0^2 = 1$ , see Eq. (16).

493 This means that in Fig. 3, the line  $\mathcal{R}_0^2 = 1$  and the separatrix between the “disease-  
494 free” and “bistability” regions meet at the point  $(u_c, a_c)$ .

495

496 **B Side results on the spatial model**

497

498 **B.1 Existence of a minimum linear spreading speed**

499 The function of the form  $\xi \mapsto \exp(-\xi s)y$  is a solution of system (3) linearised  
500 around the disease-free equilibrium if and only if  $scy = M_s y$ , in which

$$M_s = \begin{pmatrix} -\rho & \beta \\ u\theta & -1 + s^2 \end{pmatrix},$$

501 see Eq. (11). Since  $M_s$  is irreducible and, for all  $s > 0$ , essentially non-negative, the  
502 Perron-Frobenius theorem provides the existence of a unique eigenvalue  $\kappa_s$  of  $M_s$   
503 associated to a positive eigenvector [13][Theorem 1.4]. Therefore,  $sc = \kappa_s$ . Since  
504  $c = \kappa_s/s$  is the dominant eigenvalue of  $\frac{1}{s}M_s$ ,  $c$  is a convex function of  $s$  [11].

505 **B.2 Quasi-steady-state approximation**

506 In this section, we make a quasi-steady-state approximation to reduce our model to  
507 a single dimension [similarly to 26].

508 Model (3) can be equivalently expressed as:

$$\begin{aligned} \frac{1}{\rho}i_\tau &= \frac{\beta}{\rho}v \frac{a(1-i)}{a(1-i)+i} - i, \\ v_\tau &= \theta(1-v) \frac{ui}{ui+1-i} - v + v_{\xi\xi}. \end{aligned} \tag{20}$$

509 We consider the case where the infected vector removal rate ( $m + l$ ) is much lower  
510 than the removal rate of infected hosts  $r$ , so  $\rho = r/(m + l) \gg 1$ . This might happen in  
511 plant viruses if roguing occurs frequently relative to the vector lifespan ( $r \gg m$ ), and  
512 the virus is persistent in the vector ( $l = 0$ ).

513 We apply the quasi-steady-state approximation to the first equation of (20) to  
514 yield the fraction of infected hosts  $i$  directly in terms of the fraction of infected vec-  
515 tors  $v$  as

$$0 < i^\#(v) := \frac{\left(\frac{\beta}{\rho}v + 1\right)a - \sqrt{\left(\left(\frac{\beta}{\rho}v - 1\right)^2 a + 4\frac{\beta}{\rho}v\right)a}}{2(a-1)} < 1.$$

516 (It can be easily shown that the other root is greater than unity.)

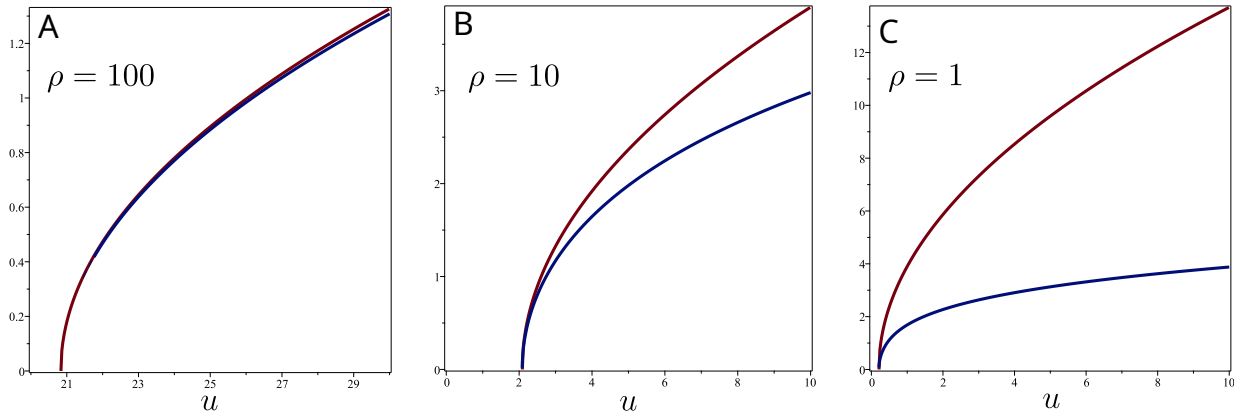


Figure 9: Exact linear spreading speed ( $c^*$ , in red), as given by numerically solving Eq. (15), and approximated linear spreading speed ( $c^*$ , in blue), as given by Eq. (23) in the monostable case. Our quasi-steady-state-approximation (QSSA) assumes  $\rho \gg 1$ . It is therefore unsurprising that the QSSA performs badly when  $\rho \leq 10$ . However, the approximation does not seem to deviate much from the exact solution for small spreading speeds and  $\rho \geq 1$ . This might explain why the QSSA correctly locates the  $c = 0$  curve in Fig. 8. Here,  $\beta = 2.4\rho$ , other parameter values as in Fig. 1.

517 This yields

$$v_t \approx \theta(1-v) \frac{ui^\#(v)}{ui^\#(v) + 1 - i^\#(v)} - v + v_{\xi\xi} =: W(v) + v_{\xi\xi}. \quad (21)$$

518

### 519 B.2.1 Monostable case ( $\mathcal{R}_0^2 > 1$ )

520 It is useful to notice that in the monostable case ( $\mathcal{R}_0^2 > 1$ ),  $W(0) = 0$ ,  $W(v^*) = 0$ ,  
 521 and  $W(v) > 0$  for all  $v \in (0, v^*)$ . It is well known that if

$$\frac{W(v)}{v} < W'(0) \quad \text{for all } v \in (0, v^*), \quad (22)$$

522 the spreading speed of the wave is linearly determined [52, 38]:

$$c^* = 2\sqrt{W'(0)} = 2\sqrt{\frac{\beta}{\rho}\theta u - 1} = 2\sqrt{\mathcal{R}_0^2 - 1}. \quad (23)$$

523

524 Fig. 9 compares the linear speed under the QSSA (Eq. (23)) with the exact linear  
 525 spreading speed given by Eq. (15). The QSSA performs well for large values of  $\rho$ , but  
 526 performs increasingly badly for smaller values of  $\rho$  that do not meet the assumption  
 527  $\rho \gg 1$  behind the QSSA.

528 Note, however, that if condition (22) is not satisfied, the spreading speed may



529 not be linearly determined. A sufficient condition for condition (22) not to hold is  
 530  $W''(0) > 0$ . We have

$$W''(0) = -\frac{2\frac{\beta}{\rho}u\theta\left((1+(u-1)a)\frac{\beta}{\rho}+a\right)}{a},$$

531 and so  $W''(0) > 0$  is equivalent to

$$u < \frac{\frac{\beta}{\rho}(a-1)-a}{a\frac{\beta}{\rho}}.$$

532 Or equivalently,

$$(u-1)\frac{\beta}{\rho}+1 < 0 \quad \text{and} \quad a > \frac{\frac{\beta}{\rho}}{-((u-1)\frac{\beta}{\rho}+1)} =: \tilde{a}(u). \quad (24)$$

533 We also have

$$\tilde{a}(u_c) = \frac{\frac{\beta}{\rho}}{\frac{\beta}{\rho}-\frac{1}{\theta}-1} = \frac{1}{1-\frac{u_c}{u^*}} = a_c,$$

534 see Eq. (19). This means that the curve separating pulled waves (linear speed)  
 535 with pushed waves (nonlinear speed) in the parameter plane “originates” at  $(u_c, a_c)$   
 536 (Fig. 10).

537

### 538 **B.2.2 Bistable case ( $\mathcal{R}_0^2 < 1$ )**

539 In the bistable case ( $\mathcal{R}_0^2 < 1$ ), the wave speed is not linearly determined. How-  
 540 ever, it is well known [21] that

$$\text{sign}(c^*) = \text{sign}\left(\int_0^{v_2^*} W(v)dv\right), \quad (25)$$

541 where  $v_2^*$  is the stable nontrivial equilibrium of (21). Hence, the travelling wave has  
 542 positive (negative) speed when the net area between the growth dynamics  $W(v)$   
 543 of the approximated system (21) and the horizontal axis in the range between the  
 544 disease-free state and the stable endemic state is positive (negative, respectively).

545 Figure 11 compares the linear spreading speed with the actual (numerically com-  
 546 puted) spreading speed under the QSSA. It shows that in the bistable case ( $u < u_c$ ),  
 547 the spreading speed can be either negative or positive. In the monostable case

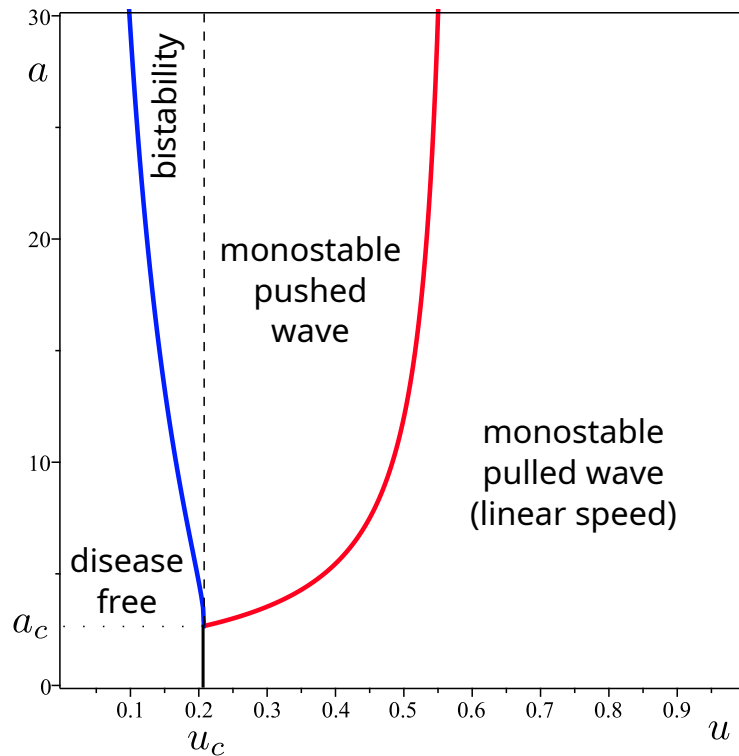


Figure 10: Two-parameter bifurcation analysis under the quasi-steady-state approximation (QSSA), i.e., model (21). The black line connecting  $(u_c, 0)$  to  $(u_c, a_c)$  is the boundary between the monostable case with linear speed and the disease-free region. The blue line separates the disease-free region from the bistability region, as given by Eq. (18). The red line separates the monostable/pushed wave from the monostable/pulled wave (linear speed) region, as given by Eq. (24). Note that Eq. (24) only depends on  $\beta/\rho$ , while Eq. (18) only depends on  $\theta$  and  $\beta/\rho$  through  $\mathcal{R}_0^2 = \beta\theta u/\rho$ . Parameter values:  $\theta = 2$  and  $\beta/\rho = 2.4$ . Note, however, that  $\rho$  must be much greater than 1 for the QSSA to hold.

548  $(u > u_c)$ , the actual spreading speed significantly deviates from the linear speed for  
 549  $u$  close to  $u_c$ , but the actual speed converges to the linear speed as  $u$  increases.

550 Figure 12 shows that the actual spreading does not depend on  $a$  when it is well  
 551 approximated by the linear speed (for  $u > 0.3$ ), while it increasingly depends on  $a$  as  
 552  $u$  decreases from  $u = 0.3$ . The dependency is greater in the bistable case ( $u = 0.15$ )  
 553 than in the monostable pushed case ( $u = 0.2$ ). As expected, the spreading speed is  
 554 non-decreasing with  $a$ .

## 555 References

- 556 [1] R. Anguelov, Y. Dumont, and J. Lubuma. Mathematical modeling of sterile insect  
 557 technology for control of *Anopheles* mosquito. *Computers and Mathematics*  
 558 *with Applications*, 64(3):374 – 389, 2012.
- 559 [2] Zhenguo Bai, Rui Peng, and Xiao-Qiang Zhao. A reaction–diffusion malaria  
 560 model with seasonality and incubation period. *Journal of Mathematical Biology*,

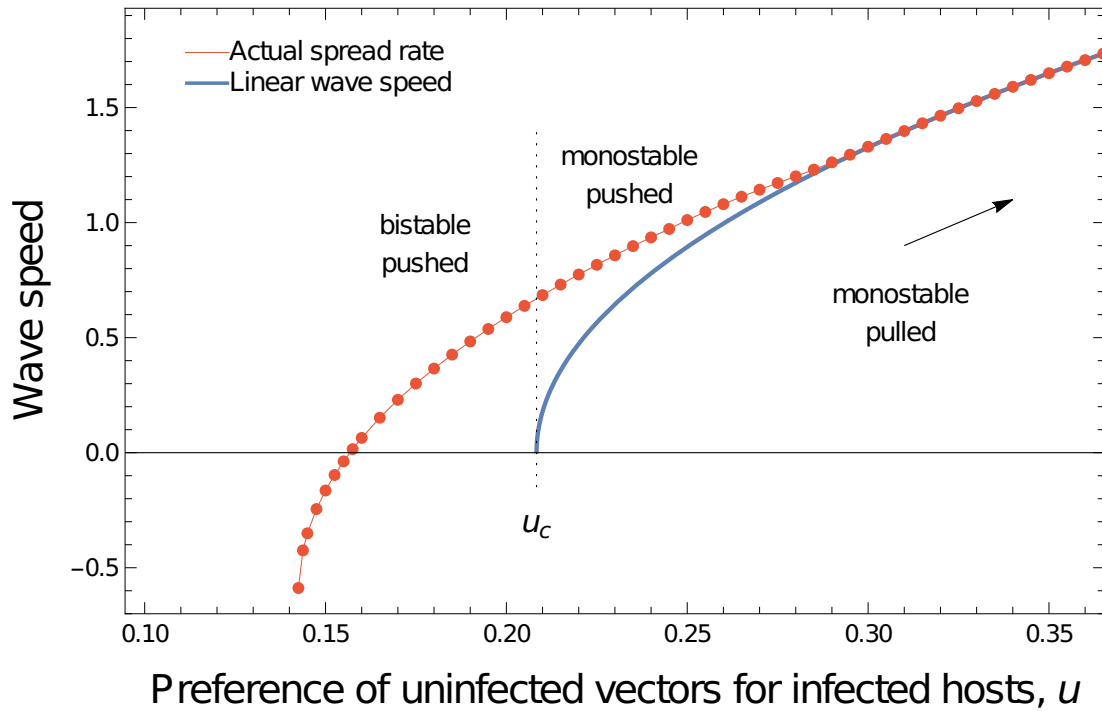


Figure 11: Comparing the linear wave speed, given by equation (23), with the actual (numerically computed) wave speed under the QSSA, i.e., model (21). Here,  $\rho = 100$ ,  $\beta = 2.4\rho$ , other parameter values as in Fig. 1.

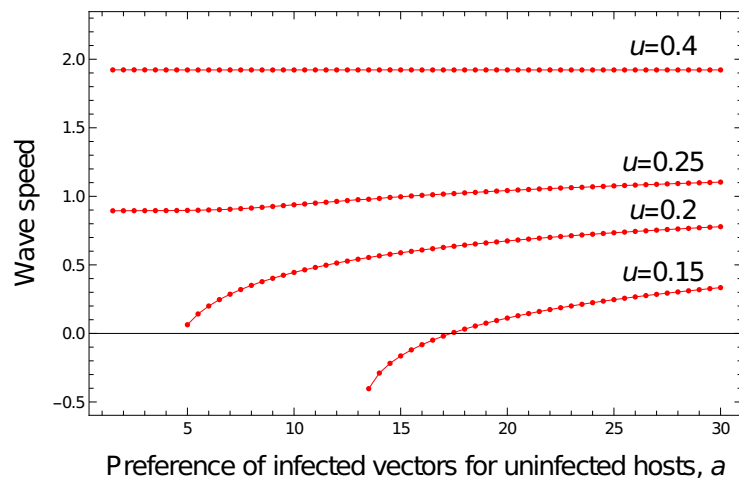


Figure 12: Shows whether and how the actual (numerically computed) spreading speed depends on  $a$ . This is for the QSSA, i.e., model (21), but the results are very similar in the original model (3), for  $\rho = 1$ . Here,  $\rho = 100$ ,  $\beta = 2.4\rho$ , other parameter values as in Fig. 1.

- 561 77(1):201–228, 2018.
- 562 [3] C. J. Bampfylde and M. A. Lewis. Biological control through intraguild predation:  
563 case studies in pest control, invasive species and range expansion. *Bulletin of*  
564 *Mathematical Biology*, 69(3):1031–1066, 2007.
- 565 [4] Andrew M Bate and Frank M Hilker. Prey-taxis and travelling waves in an  
566 eco-epidemiological model. *Bulletin of Mathematical Biology*, 81(4):995–1030,  
567 2019.
- 568 [5] Stéphane Blanc and Yannis Michalakis. Manipulation of hosts and vectors by  
569 plant viruses and impact of the environment. *Current Opinion in Insect Science*,  
570 16:36–43, 2016.
- 571 [6] Gennady Bocharov, Andreas Meyerhans, Nickolai Bessonov, Sergei Trofimchuk,  
572 and Vitaly Volpert. Spatiotemporal dynamics of virus infection spreading in  
573 tissues. *PLoS One*, 11(12):e0168576, 2016.
- 574 [7] Bruno Buonomo and Cruz Vargas-De-León. Stability and bifurcation analysis  
575 of a vector-bias model of malaria transmission. *Mathematical Biosciences*,  
576 242(1):59–67, 2013.
- 577 [8] JP Carr, T Tungadi, R Donnelly, A Bravo-Cazar, SJ Rhee, LG Watt, JM Mutuku,  
578 FO Wamonje, AM Murphy, W Arinaitwe, AE Pate, NJ Cunniffe, and CA. Gilligan.  
579 Modelling and manipulation of aphid-mediated spread of non-persistently trans-  
580 mitted viruses. *Virus Research*, 277:197845, 2020.
- 581 [9] Farida Chamchod and Nicholas F Britton. Analysis of a vector-bias model on  
582 malaria transmission. *Bulletin of Mathematical Biology*, 73(3):639–657, 2011.
- 583 [10] Michael Chapwanya and Yves Dumont. On crop vector-borne diseases. Im-  
584 pact of virus lifespan and contact rate on the traveling-wave speed of infective  
585 fronts. *Ecological Complexity*, 34:119–133, 2018.
- 586 [11] J. E. Cohen. Convexity of the dominant eigenvalue of an essentially non-  
587 negative matrix. *Proceedings of the American Mathematical Society*, 81:657–  
588 658, 1981.

- 589 [12] Stéphane Cornet, Antoine Nicot, Ana Rivero, and Sylvain Gandon. Malaria in-  
590 fection increases bird attractiveness to uninfected mosquitoes. *Ecology Letters*,  
591 16(3):323–329, 2013.
- 592 [13] E.C.M. Crooks. On the Vol’pert theory of travelling-wave solutions for parabolic  
593 systems. *Nonlinear Analysis: Theory, Methods & Applications*, 26(10):1621–  
594 1642, 1996.
- 595 [14] Nik J Cunniffe, Nick P Taylor, Frédéric M Hamelin, and Michael J Jeger. Epidemio-  
596 logical and ecological consequences of virus manipulation of host and vector in  
597 plant virus transmission. *PLoS Computational Biology*, 17(12):e1009759, 2021.
- 598 [15] Valentin Doli. *Phénomènes de propagation de champignons parasites de*  
599 *plantes par couplage de diffusion spatiale et de reproduction sexuée*. PhD the-  
600 sis, Rennes 1, 2017.
- 601 [16] Sanford D Eigenbrode, Nilsa A Bosque-Pérez, and Thomas S Davis. Insect-borne  
602 plant pathogens and their vectors: Ecology, evolution, and complex interac-  
603 tions. *Annual Review of Entomology*, 63:169–191, 2018.
- 604 [17] W. F. Fagan, M. A. Lewis, M. G. Neubert, and P. van den Driessche. Invasion  
605 theory and biological control. *Ecology Letters*, 5:148–158, 2002.
- 606 [18] Jian Fang and Xiao-Qiang Zhao. Monotone wavefronts for partially degener-  
607 ate reaction-diffusion systems. *Journal of Dynamics and Differential Equations*,  
608 21(4):663–680, 2009.
- 609 [19] Jian Fang and Xiao-Qiang Zhao. Traveling waves for monotone semiflows with  
610 weak compactness. *SIAM Journal on Mathematical Analysis*, 46(6):3678–3704,  
611 2014.
- 612 [20] Alberto Fereres, Maria Fernanda G. V. Peñafior, Carla F. Favaro, Kamila E. X.  
613 Azevedo, Carolina H. Landi, Nathalie K. P. Maluta, José Mauricio S. Bento, and  
614 Joao R.S. Lopes. Tomato infection by whitefly-transmitted circulative and non-  
615 circulative viruses induce contrasting changes in plant volatiles and vector be-  
616 haviour. *Viruses*, 8(8), 2016.

- 617 [21] Paul C Fife and J Bryce McLeod. The approach of solutions of nonlinear diffu-  
618 sion equations to travelling front solutions. *Archive for Rational Mechanics and*  
619 *Analysis*, 65(4):335–361, 1977.
- 620 [22] Sylvain Gandon. Evolution and manipulation of vector host choice. *The Ameri-*  
621 *can Naturalist*, 192(1):23–34, 2018.
- 622 [23] Karl P Hadeler and Pauline van den Driessche. Backward bifurcation in epidemic  
623 control. *Mathematical Biosciences*, 146(1):15–35, 1997.
- 624 [24] KP Hadeler and MA Lewis. Spatial dynamics of the diffusive logistic equa-  
625 tion with a sedentary compartment. *Canadian Applied Mathematics Quarterly*,  
626 10:473–499, 2002.
- 627 [25] F. M. Hamelin, Y. Mammeri, Y. Aigu, S. E. Strelkov, and M. A. Lewis. Host  
628 diversification may split epidemic spread into two successive fronts advancing  
629 at different speeds. *Bulletin of Mathematical Biology*, 84(7):1–24, 2022.
- 630 [26] Frédéric M Hamelin, Franccois Castella, Valentin Doli, Benoît Marccais, Virginie  
631 Ravigné, and Mark A Lewis. Mate finding, sexual spore production, and the  
632 spread of fungal plant parasites. *Bulletin of Mathematical Biology*, 78(4):695–  
633 712, 2016.
- 634 [27] Frank M Hilker, Michel Langlais, Sergei V Petrovskii, and Horst Malchow. A diffu-  
635 sive SI model with Allee effect and application to FIV. *Mathematical Biosciences*,  
636 206(1):61–80, 2007.
- 637 [28] Frank M Hilker and Mark A Lewis. Predator–prey systems in streams and rivers.  
638 *Theoretical Ecology*, 3:175–183, 2010.
- 639 [29] Frank M Hilker, Mark A Lewis, Hiromi Seno, Michel Langlais, and Horst Malchow.  
640 Pathogens can slow down or reverse invasion fronts of their hosts. *Biological*  
641 *Invasions*, 7(5):817–832, 2005.
- 642 [30] Geoffrey R Hosack, Philippe A Rossignol, and P Van Den Driessche. The control  
643 of vector-borne disease epidemics. *Journal of Theoretical Biology*, 255(1):16–  
644 25, 2008.

- 645 [31] Laura L Ingwell, Sanford D Eigenbrode, and Nilsa A Bosque-Pérez. Plant viruses  
646 alter insect behavior to enhance their spread. *Scientific Reports*, 2(1):1–6,  
647 2012.
- 648 [32] S Janson. Resultant and discriminant of polynomials, 2010. Unpublished  
649 manuscript.
- 650 [33] Joel G Kingsolver. Mosquito host choice and the epidemiology of malaria. *The*  
651 *American Naturalist*, 130(6):811–827, 1987.
- 652 [34] Renaud Lacroix, Wolfgang R Mukabana, Louis Clement Gouagna, and Jacob C  
653 Koella. Malaria infection increases attractiveness of humans to mosquitoes.  
654 *PLoS Biology*, 3(9):e298, 2005.
- 655 [35] M. A. Lewis and P. van den Driessche. Waves of extinction from sterile insect  
656 release. *Mathematical Biosciences*, 116:221–247, 1993.
- 657 [36] MA Lewis and G Schmitz. Biological invasion of an organism with separate  
658 mobile and stationary states: Modeling and analysis. *Forma*, 11(1):1–25, 1996.
- 659 [37] Mark Lewis, Joanna Renclawowicz, and P van den Driessche. Traveling waves  
660 and spread rates for a West Nile virus model. *Bulletin of Mathematical Biology*,  
661 68(1):3–23, 2006.
- 662 [38] Mark A Lewis and P Kareiva. Allee dynamics and the spread of invading organ-  
663 isms. *Theoretical Population Biology*, 43(2):141–158, 1993.
- 664 [39] Bingtuan Li. Traveling wave solutions in partially degenerate cooperative  
665 reaction–diffusion systems. *Journal of Differential Equations*, 252(9):4842–  
666 4861, 2012.
- 667 [40] Bingtuan Li, Hans F Weinberger, and Mark A Lewis. Spreading speeds as slowest  
668 wave speeds for cooperative systems. *Mathematical Biosciences*, 196(1):82–  
669 98, 2005.
- 670 [41] Maia Martcheva. *An Introduction to Mathematical Epidemiology*. Springer, New  
671 York, 2015.

- 672 [42] Kerry E Mauck, Consuelo M De Moraes, and Mark C Mescher. Deceptive chem-  
673 ical signals induced by a plant virus attract insect vectors to inferior hosts.  
674 *Proceedings of the National Academy of Sciences*, 107(8):3600–3605, 2010.
- 675 [43] Paul McElhany, Leslie A Real, and Alison G Power. Vector preference and disease  
676 dynamics: a study of barley yellow dwarf virus. *Ecology*, 76(2):444–457, 1995.
- 677 [44] M. R. Owen and M. A. Lewis. How predation can slow, stop or reverse a prey  
678 invasion. *Bulletin of Mathematical Biology*, 63:655–684, 2001.
- 679 [45] J. Rauch and J. Smoller. Qualitative theory of the Fitzhugh-Nagumo equations.  
680 *Advances in Mathematics*, 27(1):12–44, 1978.
- 681 [46] Jean B Ristaino, Pamela K Anderson, Daniel P Bebber, Kate A Brauman, Nik J  
682 Cunniffe, Nina V Fedoroff, Cambria Finegold, Karen A Garrett, Christopher A  
683 Gilligan, Christopher M Jones, et al. The persistent threat of emerging plant dis-  
684 ease pandemics to global food security. *Proceedings of the National Academy  
685 of Sciences*, 118(23):e2022239118, 2021.
- 686 [47] Bryan K Roosien, Richard Gomulkiewicz, Laura L Ingwell, Nilsa A Bosque-Pérez,  
687 Dheivasigamani Rajabaskar, and Sanford D Eigenbrode. Conditional vector pref-  
688 erence aids the spread of plant pathogens: results from a model. *Environmental  
689 Entomology*, 42(6):1299–1308, 2013.
- 690 [48] F. Rothe. *Global solutions of reaction-diffusion systems*. Springer, Berlin, 1984.
- 691 [49] Lauren G Shoemaker, Evelyn Hayhurst, Christopher P Weiss-Lehman, Alexan-  
692 der T Strauss, Anita Porath-Krause, Elizabeth T Borer, Eric W Seabloom, and  
693 Allison K Shaw. Pathogens manipulate the preference of vectors, slowing dis-  
694 ease spread in a multi-host system. *Ecology Letters*, 22(7):1115–1125, 2019.
- 695 [50] Mark S Sisterson. Effects of insect-vector preference for healthy or infected  
696 plants on pathogen spread: insights from a model. *Journal of Economic Ento-  
697 mology*, 101(1):1–8, 2008.
- 698 [51] H. Smith. *Monotone dynamical systems: An introduction to the theory of com-  
699 petitive and cooperative systems*. American Mathematical Society, Providence,  
700 RI, 2008.



- 701 [52] AN Stokes. On two types of moving front in quasilinear diffusion. *Mathematical*  
702 *Biosciences*, 31(3-4):307–315, 1976.
- 703 [53] Xiunan Wang and Xiao-Qiang Zhao. A periodic vector-bias malaria model with  
704 incubation period. *SIAM Journal on Applied Mathematics*, 77(1):181–201, 2017.
- 705 [54] Marjorie J Wonham, Tomas de Camino-Beck, and Mark A Lewis. An epidemio-  
706 logical model for West Nile virus: invasion analysis and control applications.  
707 *Proceedings of the Royal Society of London. Series B: Biological Sciences*,  
708 271(1538):501–507, 2004.
- 709 [55] Zhiting Xu and Yiyi Zhang. Traveling wave phenomena of a diffusive and vector-  
710 bias malaria model. *Communications on Pure & Applied Analysis*, 14(3):923,  
711 2015.
- 712 [56] Zhiting Xu and Xiao-Qiang Zhao. A vector-bias malaria model with incubation  
713 period and diffusion. *Discrete & Continuous Dynamical Systems-B*, 17(7):2615,  
714 2012.